Deciphering Mars' ancient climate from the rock record at Jezero.

For submission to ROSES – Mars 2020 Participating Scientist Program (NNH19ZDA001N-M2020PSP)

Table 1. Deciphering Mars' Ancient Climate From The Rock Record at Jezero:

Overview Of The Science Rationale For The Measurements To Be Advocated For As Part of the Proposed Investigation

Mars 2020 Science Objective	Goal of the Proposed Investigation	Key Paleoclimate Parameter	Investigation Objectives (*Mars 2020 Science Objective Addressed*)	Measurement Objectives (Tasks)	Key Measurement Requirement	Mars 2020 Payload Exceeds this Measurement Requirement (All Instruments Satisfying the Measurement Requirement Are Shown Even Where Only One Is Needed)	Science Operations Context Within Which Measurement Requirements can be Met (Sol Type from Table 6 of Mars 2020 PIP)	Science Products	Other Key Steps in Science Closure (e.g., Analyses)	Numerical Modeling Tools Available to Enhance Investigation
Addresses Mars 2020 Science Objective A " Characterize the processes that formed and modified the geologic record within a field exploration area on Mars selected for evidence of an astrobiologically-relevant ancient environment and geologic diversity, " and Objective B-1 "Determine the habitability of an ancient environment"); also "Deciphering Mars' ancient climate from the rock record" at Jezero (ROSES AO, C.26-4;	Use Mars 2020 Payload to Address Key Knowledge Gaps in Ancient Climate (How Warm Was Climate, How High was pCO2, and For How Long Did Climate at Jezero Support Habitability?)	River paleodischarge (Q) as function of stratigraphic elevation	**A.** Set Lower Limit on River Paleodischarge at Jezero. (*2020-A, 2020-B1*). B. Constrain Variability of River Paleodischarge at Jezero. (2020-A, 2020-B1, 2020-B2).	**1a.** (For gravel-bed paleochannels) Measure grain size distribution in channel deposits	D84 and D90, ±10% for 8 mm grains	SuperCam RMI (resolution 0.8 mm @ 10 m), *or*	Any	Grain-size distributions	Convert from Q (m^3/s) to runoff production (mm/hr) using drainage area A (km^2) (e.g. Irwin et al. 2005). Incorporate outcrop range information (e.g. from eng.	Accumulation-rate pipeline of Kite et al. (2017) CHIM-XPT (Palandri et al. 1998, Kite & Ford 2018, Kite & Melwani Daswani 2019) Erosion-rate pipeline of Kite & Mayer (2017) Paleoatmospheric pressure pipeline of Kite et al. (2014) ISEE-Mars (Kite et al. 2013)
						MCZ (narrow zoom iFOV 0.8 mm @ 12.3 m distance)	Any			
				1b. Measure river-deposit dimensions	Widths to ±10% Thicknesses to ±20% Radius of curvature (where visible) to ±50%	MCZ (stereo), *or*	Any	River-deposit widths, thicknesses, and radii of curvature (where visible)		
						SuperCam RMI	Any			
				1d. (For sand-bed paleochannels) Measure dune bedset thicknesses	Cross-stratified unit (bed-set) thicknesses to ±30%	MCZ, *or*	Any	Bedset-thickness data		
						SuperCam RMI	Any			
		Timescales of sedimentary crater fill at Jezero, e.g. span of suface liquid water, time gap on unconformities, cumulative duration of surface liquid water, duration of wet event.	**C1**. Set Lower Limit on the Range of Time Over Which Crater Filling Occurred at Jezero. (*2020-A, 2020-B1*). **C3.** Determine whether or not crater-filling was intermittent (*2020-A, 2020-B1,2020-B2*).	**2a.** Survey for craters that formed during sedimentary crater fill (i.e., interbedded craters)	10 cm resolution in order to identify embedded craters >10 m diameter	SuperCam RMI (resolution 10 cm @ 1 km), *or*	Any	(i) Catalog of interbedded craters. (ii) Analysis of interbedded-crater density.	Process results using analysis pipeline of Kite et al. (2017)	
						MCZ (narrow zoom IFOV 10 cm @ 1.5 km distance)	Any			
				2b. Measure paleotopography on unconformities	1 cm resolution to confirm unconformities, 10 cm resolution to trace contact.	MCZ, *or*	Any	Depth and width of corrugations in the unconformity outcrop.	Erosion-rate database of Kite & Mayer (2017).	
						SuperCam RMI	Any			
				2c. If regularly-spaced layers are present, then document their average thickness and the stratigraphic variations of this average	Average layer thickness (of regularly-spaced layers) to ±10%	MCZ	Any	Locally-averaged layer thickness at multiple stratigraphic levels	Power spectral density of the average thicknesses. Deviations from average thickness vs. strat. elevation.	
			C2. Set Lower Limit on the Cumulative Duration of Crater Filling at Jezero (*2020-A, 2020-B1*).			WATSON or PIXL	PS			
				2d. Estimate peak sediment flux (Qs)	*Same as for paleodischarge (Q) task*			Qs obtained from data on grain size, channel slope, e.t.c. (Kleinhans et al. 2010)		
		Atmospheric composition (e.g. pCO_2)	**D.** Constrain Chemistry of Water With Which Detrital Grains Interacted. (*2020-A, 2020-B1*).	**3.** Survey for detrital grains of olivine, pyroxene, carbonate minerals, and (if present) Fe-sulfide minerals	Presence/absence of detrital grains, and primary cation in carbonate grains	SuperCam VISIR	PS (all instruments), RS (SuperCam), or Approach (SuperCam) sol types	Charts of allowable combinations of pCO2, T, and pO2 on ancient Mars.	Cross plots	
						SuperCam TRR				
						SuperCam LIBS				
						PIXL				
					Diameter of resolvable detrital grains to ±20%	SuperCam RMI				
						MCZ, WATSON or PIXL				
		Weathering intensity	**E.** Constrain Relative Intensity of Physical Erosion versus Open-System Chemical Weathering at Jezero (*2020-A, 2020-B1, 2020-B2*).	**4a.** Measure weathering indices (CIA, PIA, MIA, WIS) as a function of stratigraphic elevation	Elemental abundances of Al, Ca, Na, K (for CIA, PIA), + Fe + Mg (for MIA), + Si (for WIS) to ±10%	SuperCam LIBS	Any, although most likely for the following sol types: RS, PS, or Approach (any subtype)	CIA, PIA, MIA, & WIS as a function of stratigraphic elevation.	Compare to weathering intensity data for terrestrial materials (e.g. Nesbitt & Young 1982)	
						SuperCam TRR				
						SuperCam VISIR				
				4b. Log vertical element redistribution (at e.g. unconformity, exposure surface)	Textural context for vertical element redistribution	MCZ		Elemental abundances + redistribution of elements as calculated via Ti-normalization.		
					Elemental abundances as for 4a, plus Ti	Supercam, PIXL	RS/PS (Supercam) PS (PIXL)			

Notes: If no sand-bed deposits are encountered, Task **1c** is deleted.
If no regularly-spaced layers are seen, Task **2c** is deleted.
RS = Remote Sensing, PS = Proximity Science.

Primary measurement | *Supporting or alternate measurement*

2.1. Summary, Relevance to the Mars 2020 Objectives, and Expected Significance.

The climate that allowed the Jezero deltas to form was different from the climate on Mars today. Physical and chemical traces left by that climate are used to test hypotheses about past climate on Mars. Some of these traces are best seen at the wide spatial scale allowed by orbiters, some will require the precision enabled by sample return, and many are best studied using the Mars 2020 instruments. Motivated by the potential of the rock record at Jezero to improve understanding of Mars' ancient climate, the broad goals of the proposed investigation are to constrain the warmth of the ancient climate at Jezero; determine how long was Jezero a habitable environment; and to place constraints on atmospheric composition and weathering during Jezero's crater-filling era. The proposed investigation is directly responsive to the following Mars 2020 Mission-level Science Objectives:-

- Characterize the processes that formed and modified the geologic record within a field exploration area on Mars selected for evidence of an astrobiologically-relevant ancient environment and geologic diversity (Mission Objective A).
- Determine the habitability of an ancient environment (Mission Objective B1).

The Mars 2020 PSP AO "especially encourages" investigations on "deciphering Mars' ancient climate from the rock record". The scope of the proposed investigation is to acquire and analyze paleoclimate-relevant data (e.g. grain sizes, compositional data, and fluvial deposit data) using the Mars 2020 payload. The proposed investigation would add to the case for sample return by placing candidate coring sites in the context of past habitability, climate, and climate evolution, thus supporting Mission Objective C1. The relevant Mars 2020 mission-level science objectives, the objectives of the proposed investigation, the tasks to be performed, and the relationships between tasks and objectives, are shown in Table 1. The proposed tasks are selected to provide synergy with regional-scale (e.g., upstream catchment) data and with global-scale paleoclimate-relevant datasets and numerical models (Fig. 2), thus increasing the science return from the proposed investigation.

2.2. Scientific Background.

Jezero crater records an ancient climate that permitted rivers and lakes on Mars. However, basic unknowns remain (Vasavada 2017, Haberle et al. 2017). For example, did Jezero's fluviolaustrine deposits form in a single brief pulse (Salese et al. 2019, Lapotre & Ielpi 2019) or in multiple, widely-separated phases (Mangold et al. 2018, Horgan et al. 2020)? Were the ancient rivers fed by rainfall, or by snowmelt (Wordsworth 2016, Kite 2019)? Were CO_2 levels hundreds of times greater than on modern Mars necessary for river-forming climates (Wordsworth et al. 2017)? Mars 2020 will be well-placed to address these questions. Uniquely among Mars landing

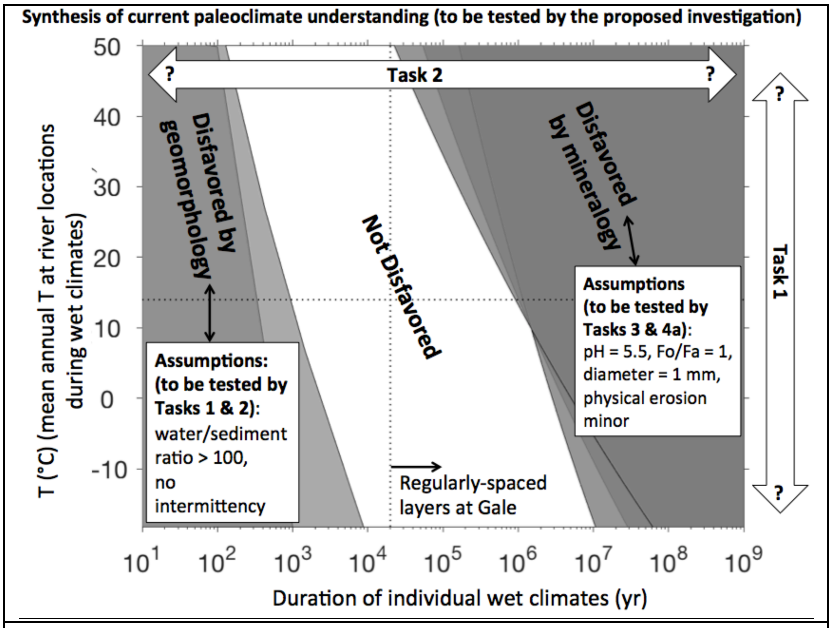

Fig. 1. Major uncertainties and untested assumptions in our current understanding of ancient climate on Mars (Kite 2019) motivate the goal of the proposed investigation.

sites, Jezero's Western Delta (JWD) encapsulates river channel deposits that drain a catchment of known drainage area (p. 5) – enabling paleo-runoff-production calculations. Moreover, Mars 2020 is targeted at the wettest climate episodes in Mars history, which offer the strongest (= best) constraints for climate models. Through integration as part of the Mars 2020 team, the proposed investigation will generate improved understanding of Jezero's habitability on timescales relevant to selection of samples for return (days to weeks), thus providing contextual information to aid in selection of samples for possible return to Earth. The proposed investigation will use the Mars 2020 payload to obtain paleoclimate-relevant data and to analyze that data to yield summary paleoclimate parameters, with the ultimate goal of understanding the warmth of Early Mars river-forming climates and for how long was the climate at Jezero suitable for life.

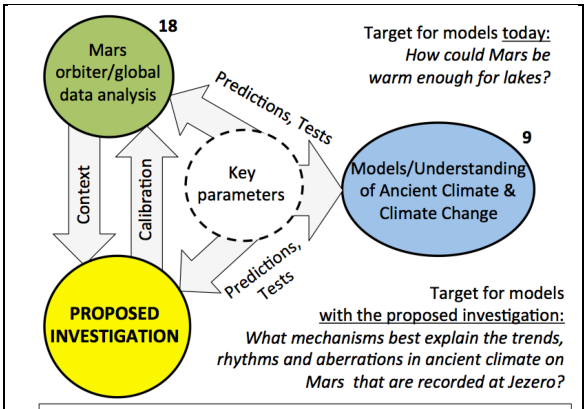

Fig 2. Relationship between models and data for ancient climate research. Through the proposed investigation and service in daily operational roles, we will work to support acquisition of samples (for possible future return to Earth) that have the greatest potential to constrain ancient climate.

Key Parameter	*Example of how this parameter can test models/hypotheses for ancient climate*	*Current Uncertainty in Parameter*	*Constraint Enabled by the Proposed Investigation*
River paleodischarge (Q)	High paleodischarge would rule out seasonal snowmelt models and would indicate rainfall on ancient Mars (Malin et al. 2010, Kite 2019)	300×	<3× (task 1)
Variability of River Paleodischarge	Seasonality and/or possible orbital variability (Metz et al. 2009) would offer new targets for climate models.	Unknown	<3× (task 1)
Range of time over which Crater Filling Occurred at Jezero	Post-impact rainout (direct conversion of bolide impact energy to water vapor) would last < 3 yr (Steakley et al. 2019, Turbet et al. 2020a).	10^7× uncertainty (20 yr – 2 Gyr); Best estimate based on untested assumptions about sedimentation rates: >(10^6-10^7) yr (e.g. Fassett & Head 2005, Schon 2012, Mangold et al 2018)	<5× uncertainty if embedded craters found, otherwise upper limit on timescale (task 2a); >5 Kyr if deep paleoyardangs found (task 2b); lower limit on regular-layer accumulation timescale (task 2c); delta build-out time constraints (task 2d)
Lower Limit on the cumulative duration of H_2O	Warming from single, isolated volcanic eruptions would last <30 yr (Halevy & Head 2014), probably less (Kerber et al. 2015). H_2/CH_4 pulses would last <10^6 yr (Tosca et al. 2018).		
Intermittency		Unknown	Strong constraints (p. 6-9)
pCO_2	~2 bar needed for CO_2-H_2 Collision-Induced Absorption (CIA) to explain rivers and lakes on Early Mars (Turbet et al. 2019, 2020b).	200× (<0.01 bar to ~2 bar); models prefer >0.1 bar	Test of ~2 bar hypothesis (task 3)
Weathering intensity	High weathering intensity strongly suggests high T (Bishop et al. 2018), or long periods with no fluvial erosion / sediment transport.	Olivine persists, but local excursions poorly constrained.	Variations in weathering intensity. (task 4)

Table 2. Examples of how geologic constraints from the proposed investigations probe hypotheses for ancient climate on Mars (Kite 2019).

2.3. Perceived impact and relevance to other NASA programs. A lot of the runoff on Early Mars came from precipitation (rain and/or melting of ice/snow) (Kite 2019, and references therein). A wetter climate, with $T > 0$ °C at least seasonally, is required to explain these observations. Explaining rivers and lakes on Early Mars is difficult because Mars 3.5 Ga received

just ⅓ of the modern Earth's insolation, which is insufficient for snowmelt and/or rain according to basic CO_2 + $H_2O_{(v)}$ greenhouse-gas models (Haberle et al. 1998, Haberle et al. 2017). Thus, the existence of rivers and lakes on Early Mars – which is the only geologic record that can give an independent test of Earth-derived models of climates that permit planetary surface habitability – shows that those basic models do not work (Ehlmann et al. 2016). Because basic CO_2 + $H_2O_{(v)}$ models do not work, recent explanations for rivers and lakes on Early Mars span a wide range of trigger mechanisms, timescales, and temperatures (Wordsworth 2016, Kite 2019, and references therein). In order to move forward in understanding Mars' ancient climate we need to test these hypotheses. (This is relevant to three of the four goals of the Mars Exploration Program, specifically the geology, climate, and search for life goals; e.g., MEPAG 2018). This requires geologists and climate modelers to coordinate. Coordination is easier if surface missions acquire data that can be integrated with global datasets and analyzed to yield quantitative summary parameters for use as input or test data for numerical models of ancient climate (Fig. 2). The proposed investigation will gather data and carry out analyses that will be maximally useful to modelers of ancient climate (Table 2).

2.4. Technical Approach and Methodology.

Our approach emphasizes measurements that can be done during the widest possible range of science operations contexts ("sol types") (Fig. 3), and with multiple instruments (Table 1). This provides operational resiliency (no one Participating Scientist investigation will drive the mission), and the flexibility to respond to unanticipated discoveries. The tasks reinforce one another and provide multiple paths to deciphering Mars' ancient climate.

2.4.1. Task 1. Constrain river paleodischarge (Q) using channel deposit grain size, bedset thicknesses, and channel-deposit dimensions.

Runoff production can be used to discriminate between snow/ice melt and rainfall on Early Mars: runoff production >3 mm hr^{-1} (adjusted for catchment area; Kite et al. 2019) would rule out seasonal snowmelt models, and imply warm planet-average temperatures and rainfall on ancient Mars (Malin et al. 2010, Palumbo & Head 2019). For channels draining topographic catchments of known area (km^2), estimates of river paleodischarge (m^3 s^{-1}) yield past runoff production (mm hr^{-1}) (Irwin et al. 2005, Dietrich et al. 2017). River paleodischarge, Q, can be obtained using data for paleochannel width, depth, slope (steeper slopes lead to faster flow), and bed grainsize (bed friction increases with grain size, slowing flow) (Hajek & Wolinsky 2012, Dietrich et al. 2017). Despite its potential, the river paleodischarge proxy has not yet yielded strong constraints on the nature of the ancient river-forming climate on Mars. MSL found fluvial gravels, but their channel width is unknown (Williams et al. 2013). Orbiter measurements of channel widths, wavelengths, and slopes have

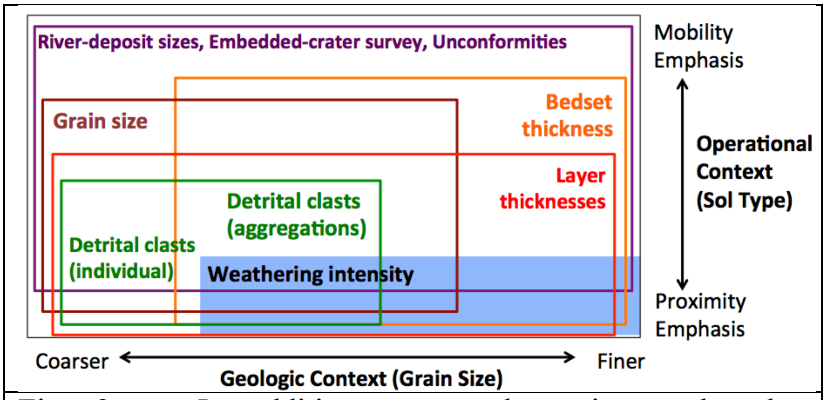

Fig. 3. In addition to complementing each other scientifically, different tasks can be emphasized depending on the geologic and operational context of the sol. Multiple tasks can be carried out in each context (Table 1). Measurement requirements can be satisfied in a wider range of contexts than shown here (Table 1). Together these attributes give the proposed investigation operational resiliency.

been used to estimate runoff production at hundreds of sites including Jezero, but bed grainsize cannot be measured from orbit (e.g. Irwin et al. 2005, Burr et al. 2010, Kite et al. 2015a, Kite et al. 2019, Hayward et al. 2019). This leads to estimates that have very large uncertainties (a factor of ~300, e.g. Fig. 3 in Kite et al. 2019), mainly because they are based on Earth-derived scalings for the relations between channel width, channel depth, and bed grainsize, that have not yet been validated on Mars' surface. These uncertainties are strongly correlated: channel depth can be estimated for self-formed channels using rover data for the grainsize of river-bed material. That is because (for gravel bed rivers) channel depth adjusts to move river-bed material downstream: the coarser the bed grainsize, the deeper (and steeper) is the channel (e.g. Parker et al. 2007, Marcelo Garcia 2008). For sand-bed rivers, similar relationships link preserved-dune-bedform (bedset) height to total river depth (e.g. Bradley & Venditti 2017). The combination of grainsize and depth information gives the best discharge estimates, with uncertainty of a factor of 3 or even better (Eaton et al. 2013). Mars 2020's payload can measure paleochannel deposit dimensions (a proxy for paleochannel dimensions) and grainsize at Jezero. JWD drained a topographic catchment area of $1.2\pm0.2 \times 10^4$ km^2 (Goudge et al. 2015, error due to Hargraves ejecta). Moreover, JWD preserves river channel deposits at multiple stratigraphic levels including near the topographic base of JWD (e.g. Goudge et al. 2018). Thus, through Mars 2020's payload, we can constrain Q at JWD. Bed grainsize (and channel width) measurements at JWD can be used to benchmark and calibrate global databases of paleohydrologic parameters (e.g., channel width), increasing the science payoff from the proposed investigation.

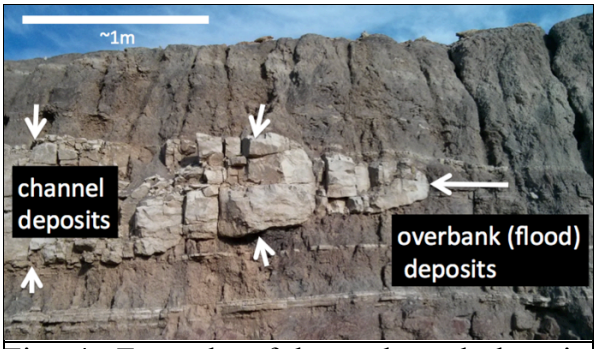

Fig. 4. Example of how channel deposits (white arrows) may be distinguished from non-channel deposits. 38.927°N 110.363°W (W of Green River, Utah).

Task 1a. River channels can be gravel-bedded or sand-bedded (Task 1c). We expect JWD channel deposits to contain gravel, by analogy to Gale, and by analogy to Earth rivers of similar slope (1%) and length (50-200 km). We will measure coarse channel deposit grain size using Mastcam-Z images. At Bradbury Landing, MSL Mastcam (spatial resolution ≈ that of Mastcam-Z) was used to measure gravel grain size ranges from 4 mm to 8 mm (Dietrich et al. 2017). For gravel-sized bed particles, ≥100 clasts must be measured from the channel deposit of interest (Kondolf 1997). Grains down to 1 mm in size will be well-resolved by Mastcam-Z (~0.13 mm/pix iFOV at 2 m for narrow zoom) and/or SuperCam RMI, which has similar effective resolution. The outline of each clast shall be traced to form a polygon with area A, and clast diameter (D) reported as $(4A / \pi)^{0.5}$. For clasts whose outline is partly occluded, a circle will be fit using least-squares to points traced along the visible part of the arc and the D for that circle reported. Results for analysis using automatic procedures (e.g Buscombe 2008) will also be reported, however the automatic procedures will not be used as a substitute for manual tracing and the manual tracing methods will be used as the gold standard for subsequent analysis. The average range to the outcrop, needed to convert D from pixels to physical units, can be obtained from stereo imagery with Mastcam-Z or from engineering camera data. Uncertainty of ±10% in clast diameter is acceptable because of ±50% uncertainty in conversion from channel dimensions / grainsize to paleodischarge. Therefore, it will usually not be necessary to track small within-image variations in range to target. Finally, grain size will be used to estimate Q following the scalings of Parker et al. (2007) as applied to Mars by Dietrich et al. (2017). Grain size measurements to constrain paleodischarge Q (addressing Investigation Objectives A/B) also support Investigation Objective

C (by constraining sediment discharge Q_s). Grainsize information can be used to estimate Q as was done at Gale (Dietrich et al. 2017), and constraints on Q are stronger when grainsize information is combined with paleochannel deposit dimensions (Task 1b).

Task 1b. The thicknesses, and where visible the widths, of paleochannel deposits will be logged using stereo Mastcam-Z images (Fig. 4). This will, for the first time, allow from-orbit paleochannel width estimates (which might be overestimates due to possible amalgamation of channel deposits) to be checked. River depth estimated using thickness of channel deposits / clinoforms (a proxy for channel depth; Mohrig et al. 2000) can be compared to river depth estimated using the threshold channel approach in Task 1a (Pfeiffer et al. 2017). Another cross-check on width-derived paleodischarge is paleodischarge estimated from the plan-form correlate between meander wavelength and discharge (e.g. Irwin et al. 2015) (Fig. 5). Sinuous river deposits have been identified from orbit at Jezero (Goudge et al. 2018) and so river-deposit curvature can be ground-truthed (and extended to additional meander deposits not seen from orbit) with Mastcam-Z stereo observations. Paleochannel deposit dimensions from rover data give a more precise estimate of Q than does plan-view paleochannel morphometry as seen from orbit, because of the added dimension of deposit thickness. The best constraints come from combining paleochannel deposit dimensions with grainsize information (Task 1a) (Hajek & Wolinsky 2012).

Task 1c. If sand-bedded river deposits are encountered, then an alternative method of channel depth estimation can be used. The height of the deposits of dune bed-sets is a proxy for the depth of the river channel (e.g. Hajek & Heller 2012, Hayden et al. 2019), multiplied by 3.5 (95% confidence interval: 2.2 – 9.9) to correct for incomplete preservation (Leclair & Bridge 2001, Bradley & Venditti 2017). We will supplement this by direct measurement of paleochannel fluvial bar clinoforms in outcrops where both the top and bottom of such clinoforms can be seen (Mohrig et al. 2000). If no sand-bedded river deposits are seen, Task 1c is deleted.

Stratigraphic Approach to Task 1 (Fig. 5). Climate events in Earth history are recorded in fluvial sediments through changes in channel dimensions and bed grainsize (e.g. Foreman et al. 2012). Paleodischarge estimates for different stratigraphic levels on Mars can be combined to obtain changes in runoff production over time. HiRISE data show channels at JWD at multiple stratigraphic levels. Therefore, logs of data gathered via Tasks 1a-1c can answer the question "What does the Jezero stratigraphy tell us about early Mars valley network hydrology and erosion?" Did runoff wane over time, was it periodic, or was it pulsed? Data from the proposed investigation will be referenced to a stratigraphic elevation interpolated from marker surfaces (following Kite et al. 2015a) (Fig. 5). In order to construct reference stratigraphic surfaces, we will correct absolute

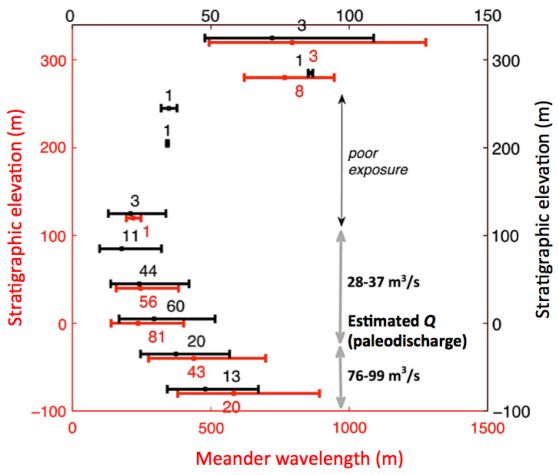

Fig. 5. (From Kite et al. 2015a). Logs of paleohydrologic parameters using orbiter data at Aeolis Dorsa, Mars. Error bars show 1σ spread of measurements (averaged in 40 m z_s bins). Numbers next to error bars correspond to the number of measurements. Estimates of Q from width (w) and wavelength (λ) methods agree within error. Mars 2020's payload enables higher stratigraphic resolution, and greater confidence in Q estimates.

elevations for layer tilts (0-8° at JWD, Goudge et al. 2017; we will use tilts >3° as a screening tool to exclude foresets) as we have done previously (e.g. Kite et al. 2015a, Kite et al. 2016). Task 1 Uncertainties and Limitations. The largest pre-landing unknown is whether channels are gravel-bedded or sand-bedded. This uncertainty is fully mitigated by the complementarity of Task 1a (gravel) and Task 1c (sand). River deposits, especially in small catchments, record infrequent floods. This limitation is acceptable, because maximum runoff production, corresponding to floods, is the most useful test for climate models.

2.4.2. Task 2. Constrain the time span(s) of crater fill at Jezero using observations of interbedded impact craters, disconformities / unconformities, layer counts, and other methods.

For how long was surface liquid water present at Jezero? Estimates range from 20 yr up to a total time span of ~10^9 yr (Fassett & Head 2005, Mangold et al. 2018, Ramirez 2017, Horgan et al. 2020). It is thought that the mafic (possibly volcanic) floor unit (Shahrzad et al. 2019) is much younger than the other units, but this hypothesis is untested. Refining estimates for the duration of surface water availability at Jezero crater will inform where Mars 2020 should preferentially search for biosignatures (Mission Objective 2B). For example, if liquid water was only briefly available (e.g., 10^2 years), Jezero's lacustrine deposits would be less likely to record potential paleohabitats than more ancient materials from the upstream catchment. In this scenario, the fluvially processed ancient material would be the preferred target for seeking Martian biosignatures, rather than the lake deposits. Timescales of interest at Jezero include the total time span of surface liquid water, (τ_1); time gaps at unconformities (τ_2); the cumulative duration of surface liquid water (τ_3); and the duration of an individual wet event (i.e., the time elapsed without a dry spell lasting decades or longer) (τ_4). The sedimentary rock record constrains these timescales, in part because at least some liquid water is involved in induration via aqueous cementation. Together, these timescales define the intermittency of surface liquid water at Jezero (Fig. 6) (we hypothesize that a record of multiple wet-dry cycles will be found preserved at Jezero). All of these sedimentary-rock-record constraints are essentially lower limits; stratigraphy is an incomplete record, at any one site. Mars 2020's payload can constrain these habitability-relevant parameters through the tasks described below.

Task 2a. Survey of interbedded craters. Craters embedded within ancient sedimentary deposits are common on Mars (e.g. Edgett & Malin 2002) and have been used to constrain sedimentation timescales (e.g. Kite et al. 2013) – the longer the duration of sediment accumulation, the more craters will be found embedded within the ancient sediments. Our existing pipeline for converting embedded-crater survey data into sedimentation duration (Kite et al. 2017) takes account of uncertainty in crater flux during sedimentation (e.g. Hartmann, 2005); target strength (e.g. Dundas et al. 2010); paleo-pCO_2 (Kite et al., 2014); and Poisson error, among other factors. Combined uncertainty in duration is about a factor of five (Kite et al. 2017). As an example without uncertainty propagation, suppose intermittent fluvial activity at Jezero started at 3.6 Ga and that the youngest exposed fluvial/lake deposits at Jezero date to 3.4 Ga. Using the chronology function of Michael (2013), approximately 4,000 craters with diameter >16 m would then be interbedded within a ~20 km^2 area of Jezero Western Delta (JWD). Some of these craters will be exposed at the surface

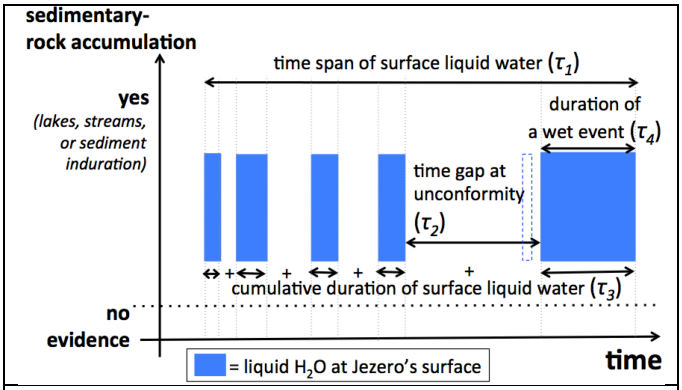

Fig. 6. Timescales of interest for Task 2.

today. Rover data are needed because it is easy to overlook small interbedded craters in orbiter images (Kite et al. 2013, Grotzinger et al. 2011). Crater fill at Jezero began at a time when the crater flux at Mars was much higher than the flux today, and may have extended over 2 Ga (Fassett & Head 2008, Sharhzad et al. 2019), increasing the density of interbedded craters. The data needed to carry out this survey are Mastcam-Z and/or SuperCam images capable of resolving 10 m diameter craters embedded in sedimentary strata. We require 10 cm resolution, giving ≥100 pixels across target. This is sufficient for identification of features as definitely impact craters that are definitely embedded within the stratigraphy (Warren et al. 2019). The 10 m threshold is set assuming that the Mars atmosphere was capable of screening smaller craters (the smallest hypervelocity crater on Earth, the 2007 Carancas impact in Peru, is 13.5 m diameter). If still smaller impact craters are found at Jezero, then we will use our existing pipeline to find an upper limit on paleopressure (Warren et al. 2019). We will plan/advocate for imaging of horizons at which we expect a high probability of interbedded craters, for example: 1. the contact between the delta and the floor unit; 2. the contact between the lower point bars and the upper channels; and 3. the contact between the mafic floor unit and the light-toned floor. In addition, we will plan/advocate for additional imaging of any other stratigraphic levels at which embedded craters are found. The following criteria (among others), modified from our orbital analysis workflow, will be used to identify embedded craters. 1. Bowl shape, truncation of pre-existing strata. 2. Preservation of a rim. 3. Fracturing below and surrounding the impact crater. 4. Onlap of subsequent sediments. Taking account of geometric and other corrections, we will convert our survey results into constraints on the time over which the delta built up, using our existing pipeline (Kite et al. 2017). As with all Mars crater chronology methods, the interbedded crater method uses a Moon-to-Mars correction factor (Michael 2013) that is uncertain by a factor of two or more (Cohen et al. 2019). This limitation is acceptable for Task 2a because uncertainty in the duration of fluviolacustrine activity greatly exceeds the uncertainty in crater flux. If, unexpectedly, no interbedded craters are found at Jezero, that would imply (a) that fluviolacustrine activity at Jezero was brief relative to the history of ancient Mars, an important constraint on habitability; and (b) that radiometric ages for any igneous materials in the mafic floor unit are close in age to that of the delta. Three other tasks (2b-2d) provide alternate routes to closure on investigation objective C (Table 1).

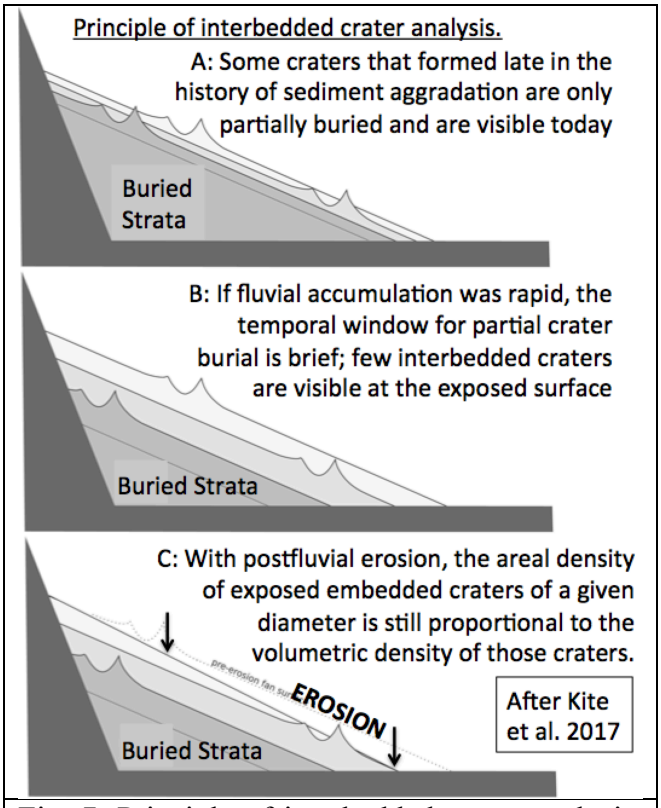

Fig. 7. Principle of interbedded crater analysis. This method has been applied to Mars river deposits by Kite et al. (2013, 2014, 2017), who found >100 such craters, almost all with diameter >100 m.

Task 2b. Paleotopography analysis. We will measure the paleotopography on unconformities whose outcrop expression is consistent with >km horizontal extent (e.g. the sub-Grasberg surface at Meridiani; and the sub-Stimson surface at Gale, Banham et

al. 2018). We will first trace the contact on Mastcam-Z mosaics. We will also report qualitative constraints on the direction of any preferred alignment of erosion features. We will check for strata distortion above the unconformity, which might indicate differential compaction (Lefort et al. 2012, Gabasova & Kite 2018). Paleotopographic data can be used to identify processes in Jezero's geologic evolution, which in turn can be used to infer paleoclimate conditions. For example, deep <300m-wavelength corrugations (Banham et al. 2018), e.g. paleoyardangs, indicate wind scour by saltation abrasion of indurated materials (Grotzinger 2014, Farley et al. 2014). Saltation abrasion implies an arid to hyperarid climate interval (little or no liquid water at surface). Alternatively, a smooth surface truncating strata at a low angle with >km horizontal extent indicates aeolian deflation of water-altered surface materials (Shao 2008) *or* pedimentation involving overland flow. Both processes imply a semiarid to arid climate (occasional liquid water at surface). Fluvial incision at an unconformity surface indicates paleolake level fall (increase in ratio of evaporation to precipitation), or lake breaching. Additional methods of determining geologic processes at unconformities includes the presence/absence and size/angularity of any rip-up clasts (fluvial vs. aeolian erosion); and the draping vs. onlapping relationship of overlying strata (fluvial vs. aeolian infill). Paleotopography analysis can also suggest erosion timescales. Saltation abrasion rates on Mars are <0.1-1 μm/yr, and on Earth are <1 mm/yr (e.g. Grindrod et al. 2014, Kite & Mayer 2017, Golombek et al. 2014). Therefore, a 5 m deep paleoyardang would suggest an arid interval lasting >5 Kyr, and more likely 5-50 Myr. Finally, because unconformities at Jezero record times of relative dryness, their analysis may constrain the number of lacustrine sequences.

Task 2c. Layer thickness analysis. At Gale, MSL discovered regularly-spaced, mm-scale layers, etched out by wind erosion, and interpreted by the MSL team as varves (annual layers) (Rubin et al. 2015, Grotzinger et al. 2015). At Gale, this indicates a total duration of surface liquid water of $>2 \times 10^4$ yr, perhaps >300 Kyr (possibly including intermittent drying-out; Fedo et al. 2017, Stein et al. 2018). At Jezero, we expect to encounter regularly-spaced layers in fine-grained distal deltaic or lacustrine sediments (e.g., light-toned floor unit, JWD outliers, JWD bottomsets). If Mars 2020 finds regularly-spaced layers at $10^{-3} – 10^0$ m scale at Jezero, then we shall analyze the thickness of such layers. The MSL team used visual inspection of layers at Gale to document stratigraphic variations in average layer thickness (Hurowitz et al. 2017). Our approach is similar. We will make measurements on images (e.g. Mastcam-Z) with resolution sufficient to resolve individual layers, with the distance between layers counted over ~10 layers, such that the mean thickness of layers within that set is constrained to ±10%. Viewing-angle and stratigraphic-tilt corrections will be made using stereo data from Mastcam-Z or engineering cameras. The PI has previously led a large study measuring Mars stratigraphic-tilts using stereo data (~300 layers) (Kite et al. 2016). We will use geologic context (e.g. grainsize, onlap vs. draping relationships at geologic contacts, composition, and the presence/absence of grading), to distinguish between the orbital and annual hypotheses for the pacemaker of regular layering (Lewis & Aharonson 2014). Outcrop thickness divided by mean regular-layer thickness is a lower limit on the time span of liquid water, because more-than-annual spacing of layers of regular thickness is plausible, but processes that produce layers more than once per warm season tend not to produce regular layers (Stack et al. 2013). Quasi-periodicity will be validated using the specific tests of Lewis & Aharonson (2014). For the purposes of this investigation, more complicated approaches (e.g. wavelets) are unnecessary. In zones where regular layering is found, we will advocate for spot-checks for unresolved (very close-spaced) layers using WATSON. If such spot-checks are not possible, our results will still serve as a lower limit and thus close objective C2. Because layer thickness variations have proven to be proxies for paleoclimate variations for regularly-spaced layers on Earth (e.g. lake varves, e.g. Moore et al. 2001, Olsen et al. 2019), the proposed layer

thickness dataset would also be used to calculate the power spectral density of layer thickness variations. The power spectrum of Earth's long-term climate is constrained by the power spectral density of paleoclimate proxies including layer thickness distributions. For Earth, at-a-site variability on timescales of decades to many Kyr is well fit by $P(f) \propto f^{-b}$, where P is spectral energy, f is frequency, and b = 0.6-1.3 in the tropics (Huybers & Curry 2006). This implies a capacitor in Earth's climate system with >Kyr thermal "memory". On Earth, this capacitor is an ocean. Thus, local fluctuations in the thickness of regularly-spaced layers can probe regional-to-global climate. We will plan/advocate for image mosaics and images at a range of spacings (e.g. meters of stratigraphic separation, versus tens of meters) in order to compute the power spectral density of deviations from the mean layer thickness. Constraints on the power spectrum of deviations from regularity in regularly-spaced layers on Mars would be valuable for ancient Mars climate research.

Task 2d. Sediment flux estimate. Some Hesperian deltas in closed-basin lakes have been proposed to have lasted $>(10^2 - 10^3)$ yr, based on delta volume and assuming water:sediment ratio ≥100:1 (Irwin et al. 2015, Palucis et al. 2016, Williams & Weitz 2014). However, this water:sediment ratio assumption has never been checked on Mars. Low water:sediment ratio flows (sediment concentration >200 kg m^{-3} has been measured during floods for the Yellow River; Ren & Shi 1986), could build out deltas in $<10^2$ yr (e.g. Kleinhans et al. 2010, Mangold et al. 2012). The grain size and paleohydraulic analysis to be carried out for Task 1 also constrains peak fluvial sediment flux (Q_s, m^3/s). The measurements to be obtained for this task are the same as for the paleodischarge task. We will use standard bedload and suspended load relations (as compiled in Kleinhans 2005), for example the Meyer-Peter Müller equation and the Van Rijn equations (substituting the high-efficiency-regime equations of Ma et al. 2020 if grainsize is <80 μm), to obtain peak Q_s from the grain size measurements and paleohydraulic analysis from Task 1a. JWD may record a closed or open basin lake. In either case, division of Q (from Task 1a) by Q_s would provide new constraints on water:sediment ratio and thus delta build-up time.

Box 1. Modeling Tools Available to Enhance Investigation & Add Value to the Science Mission.
The PI is an experienced user of a number of modeling tools that are available to inform and supplement the investigation, e.g. *ISEE-Mars (a meltwater production model; Kite et al. 2013b), *embedded crater analysis pipeline (Kite et al. 2014/2017), *erosion rate pipeline (Kite & Mayer 2017), and the reaction-transport code CHIM-XPT (Reed 1998, Kite & Ford 2018), among other tools. Tools marked "*" were built by the PI, and will be made open-source as part of the proposed investigation (Data Management Plan). Each tool can reliably generate results on operational timescales (hours or overnight, including setup time). These tools will be available both to augment our own investigation, and to assist with mission/science operations. *Scenario #1:* Analysis of a weathering profile (Task 4b) leads to a snowmelt rate estimate. Convolution of this estimate with standard fluvial sediment transport equations (Task 2d) leads to prediction of debris flow deposits at this stratigraphic level. PI plans/advocates for imaging to test prediction. *Scenario #2*: STG requests analysis of likelihood of preservation of complex organic matter at a proposed drill site. PI uses abundance of small craters to assess likelihood for preservation of complex organic matter using Kite & Mayer (2017) pipeline, thus addressing Mission Objective B2.

2.4.3. Task 3. Analyze detrital clast composition, shape, and size.

Background. Jezero's deltas, which formed by detrital sedimentation, still contain a large fraction of detrital phases (Horgan et al. 2020, Goudge et al. 2017). Olivine is abundant in the delta, and because olivine does not survive pervasive and long-lived aqueous alteration, authigenic resetting of the initially detrital composition of JWD cannot be complete. Consistent with detrital

reworking, the mineralogy of the JWD, including alteration phases, is generally similar to that of the JWD source region based on CRISM analysis (Goudge et al. 2015), although small outcrops of likely-authigenic phases also exist (Tarnas et al. 2019). Carbonates at JWD are concentrated in point bar strata, consistent with a detrital origin. Upstream of JWD, olivine+carbonate bearing materials overlie pyroxene+smectite materials (Mandon et al. 2020). However in the JWD, pyroxene/smectite bearing materials near the top of JWD are underlain by olivine+carbonate bearing strata. Tectonic faulting is not a reasonable explanation for this observation, so this stratigraphic inversion at JWD can be explained only if high-standing units in the catchment were eroded earlier and so were deposited lower in the delta. In turn, this implies that most of these specific mineral phases in JWD are detrital (Goudge et al. 2015, Horgan et al. 2020).

Detrital material in JWD has been weathered, eroded from the watershed to the west of Jezero, and transported by rivers. Thus, clasts were subject to abrasion and dissolution. (Once deposited and buried, clasts enter more rock-buffered conditions where dissolution may be much slower). The rate of dissolution for a given mineral depends on environmental conditions, for example pH and pO_2 (Johnson et al. 2014). For example, olivine persistence is frequently used to set upper limits on the duration of Mars aqueous alteration (e.g. Hausrath et al. 2008). This dependence of dissolution rate on environmental conditions is especially strong for minerals such as pyrite, and siderite (among other minerals) that are unstable at low pH and/or high pO_2. Therefore, the composition and size of detrital grains has been used for >30 years as a basic probe of ancient river water chemistry and of atmospheric composition (Holland 1984, Rasmussen & Buick 1999, Johnson et al. 2014, Catling & Kasting 2017). On Mars, burial of carbonates could be an important sink for CO_2 (Franz et al. 2020). The link between river water chemistry and atmospheric composition is that (in contrast to lake water), river water is fresh. The implications for Early Mars river water chemistry can be illustrated as follows. Suppose the Early Mars atmosphere had $pCO_2 = 2$ bar. This is the pCO_2 needed for strong greenhouse warming according to the H_2-CO_2 Collision-Induced Absorption hypothesis (Turbet et al. 2020a). We adopt the modern Earth river rock:water ratio, which is $10^{-4.4}$ to $10^{-4.0}$ mol kg^{-1} H_2O (Berner and Berner 2012, Hao et al. 2017). Then, the water's pH ≈ 4 with a 0.13 M concentration of C species (Drever 1997, Kite & Melwani Daswani 2019). Under these high-pCO_2 conditions, the pH of precipitation-fed rivers on ancient Mars is essentially atmosphere-buffered, set by atmospheric pCO_2 and pSO_2 (Bullock & Moore 2007). By assuming $pSO_2 = 0$, we obtain an upper limit on atmospheric pCO_2. Similar reasoning allows constraints on pO_2, pSO_2, and (less stringently) T.

Measurement plan. We will (i) determine size of detrital grains; (ii) confirm (or reject) the hypothesis that the phases are in fact detrital, (iii) measure composition of detrital grains. (i) Size. Dissolution is proportional to the ratio of effective surface area to volume. Diameter precision of ±30% is sufficient, because of greater uncertainties elsewhere in the calculation. This will be measured with Mastcam-Z and/or SuperCam RMI using a workflow similar to that for Task 1a. If grains are very small, we will use upper limits on grainsize, and/or advocate for a PIXL or WATSON spot-check. As a supplemental check, where appropriate LIBS data will be used to calculate the point-to-point Gini index of major element oxides (G_{MEAN}) using the Gale-tested protocol of Rivera-Hernández et al. (2019). (ii) Detrital origin. Criteria for assessing whether or not grains are detrital include (a) Grain shape, e.g. circularity and convexity. (b) Grain boundaries correspond to a change in outcrop color or composition (as a check for mineral replacement). (c) Strong sedimentological control of grain distribution (e.g. concentrated on bedding planes). Additional criteria applied to Archean detrital grains by Rasmussen & Buick (1999) will also be used. (iii) Composition. Most minerals of interest for this task (olivine, pyroxene, pyrite) can be identified using Mastcam-Z and/or SuperCam data (Maurice et al.

2020), either targeting aggregates of grains, or individual clasts. For carbonates, it is difficult to deconvolve the atmospheric CO_2 signal from mineral C in LIBS data. Therefore, identification of magnesite, hydromagnesite, siderite and dolomite might require time-resolved Raman (TRR) mode on SuperCam (which works best with coarse-grained materials), VISIR, or both. Relative to the other sub-tasks in the proposed investigation, these carbonate measurements are relatively time-consuming (e.g. 16 min for a 48-point, 3-spectal VISIR); however, carbonates are a major focus of interest for the Mars geoscience community (e.g. Horgan et al. 2020, and references therein). SuperCam VISIR has dedicated tables for 2.5-μm, 2.3-μm, 1.9- μm and 1.4-μm rapid sampling (Maurice et al. 2020). The spot size of TRR/VISIR is larger than for LIBS, so on/off sampling may be needed to check for carbonate spectral features. The mineral diagnosis capabilities of SuperCam are significantly greater than those of ChemCam . The Fo/Fa ratio in detrital olivine is of particular interest, because Fa dissolves ~6× faster than Fo (Olson & Rimstidt 2007). Textural and mineralogic context will be used to distinguish detrital carbonate from authigenic (or "reworked", i.e. dissolved and reprecipitated) carbonate. For each site where detrital grains can be resolved (either as individual clasts or as aggregates of unresolved clasts), we will first document size, detrital origin, and mineralogy for olivine; pyroxene; and carbonates, if these turn out to be detrital. We will also use Mastcam-Z images to search for other candidate detrital minerals, and plan/advocate for SuperCam confirmation. For example, reports of akaganeite at JWD (Dundar et al. 2019) suggest that pyrite/pyrrhotite was present in the Jezero catchment (Carter et al. 2015). Candidate detrital pyrite/pyrrhotite would show up as dark-toned grains of a locally smaller grain-size. Redox-sensitive detrital minerals, if present, would enable tests of hypotheses, e.g. (1) that O_2 levels were high early in Mars history (Lanza et al. 2016), or (2) that $pH_2 > 50$ mbar for warm climates on ancient Mars (Wordsworth et al. 2017). If detrital grains are found in Mastcam-Z images to have color variations suggestive of ancient weathering rinds, then we will also advocate for PIXL transects across candidate rinds. Weathering rinds may constrain ancient paleoatmospheric composition (e.g. Hessler et al. 2004).

Analysis plan. During fluvial transport on Mars, grains are tumbled in fresh water, and pervasive organic-matter coatings are unlikely because of low organic-matter abundances (Eigenbrode et al. 2018); thus, laboratory-measured dissolution rates are relevant to dissolution during fluvial transport on Mars. To get from observations of detrital grains to constraints on river chemistry (e.g. pH and/or river dissolved pO_2), we will use standard compilations of the dependence of dissolution rate on pH, pO_2, DIC, and other parameters (e.g. Palandri & Kharaka 2004, Morse & Arvidson 2002). To link dissolution-rate data to grain survival, we will consider a span of net sediment transport rates from 0.5 m/yr (corresponding to long residence time in floodplains; Carretier et al 2019) up to 300 m/yr (corresponding to directly-downstream sediment transport with no intermediate floodplain storage; Sinclair et al. 2019). As a cross-check of transport distances inferred from orbiter data (e.g. Goudge et al. 2015), the circularity and convexity of pebbles will also be measured using the Szabó et al. (2015) convex-hull protocol, and analyzed to obtain transport distance using the procedure applied to Bradbury Landing by Szabó et al. (2015). Finally, to link pH to atmospheric conditions (e.g. pCO_2), we will use look-up tables for ancient Mars CO_2-H_2O-basalt and CO_2-H_2O-olivine reaction from our previous work (Kite & Melwani Daswani 2019). These tables span pCO_2 = 0.006-6 bars and were computed with reaction-transport / thermodynamic equilibrium program CHIM-XPT (Reed 1998). Additional CHIM-XPT runs (e.g., varying pO_2) will be carried out as motivated by Mars 2020 observations. We do not propose to use the absence of any specific detrital mineral as a paleoenvironmental constraint. This is because such absence could be due to burial diagenesis instead of (or in addition to) surface weathering. *Example:* The Jezero delta contains magnesite based on CRISM analysis (Horgan et al. 2020, Brown et al. 2020). For the purpose of giving an example of our

analysis procedure, we suppose that 4 mm diameter grains of detrital magnesite (84.3 g/mol) are observed in the Jezero delta. Surface area is 0.50 cm^2. The corresponding lifetime against dissolution is 210 years at pH = 4.5 (Pokrovsky et al. 2009), including the stabilizing effect of high DIC. This is short compared to pre-landing best-estimate sediment transport timescales (Schon et al. 2012). We will constrain these timescales independently via tasks 2a-d, but if pre-landing estimates hold up, then detrital magnesite would place an upper limit on pCO_2 on ancient Mars. Such a constraint would disfavor the H_2-CO_2 CIA warm-climate hypothesis (Table 2). Results obtained from analysis of different mineral types can be used as an internal cross-check on inferences about ancient water chemistry.

2.4.4. Task 4. Collect and analyze data to make stratigraphic logs of open-system alteration. The contrast between the evidence for paleolakes on Mars, versus geochemical evidence for generally low water-rock ratios, is "[a] fundamental paradox" (McLennan 2012). Ideas suggested to resolve this apparent paradox include (i) that ancient Mars was cold (Fairen et al. 2011), and (ii) that climate alternated between arid and river-forming states (Sagan et al. 1973, Ehlmann et al. 2016). At Jezero, Mars 2020's payload can provide ground truth for whether or not Jezero records high water-rock ratio alteration, using the methods described below.

Task 4a. Measure weathering indices (CIA, WIA, MIA, WIS) as a function of stratigraphic elevation in sediments. What does the chemistry of rocks/regolith at Jezero tell us about near-surface chemical weathering on Mars? River sediments on Earth have a composition that responds to the climate, bedrock composition, and tectonic setting of the watersheds that those rivers drain (e.g. Nesbitt & Young 1982). For example, the Chemical Index of Alteration, CIA (= Al_2O_3 / (Al_2O_3 + CaO* + Na_2O + K_2O) ×100; excluding Ca from carbonates and sulfates; essentially a feldspar weathering scale) varies from 50 for the St. Lawrence River, to 90 for the Congo River. The extent of alteration is a measure of the relative intensity of physical erosion and open-system chemical weathering. Alteration indices can be used to estimate the extent of alteration (although all alteration indices have limitations, as discussed below). If physical erosion is fast relative to open-system chemical weathering, then CIA reflects protolith composition. If the long-term average rate of physical erosion is slow relative to open-system chemical weathering, then CIA rises. At Gale, rocks sampled early in MSL's mission show low CIA consistent with no open-system alteration (McLennan et al. 2014). Mudstones sampled later in MSL's mission show modestly elevated CIA, consistent with some open-system alteration (Mangold et al. 2019; qv. Bedford et al. 2019). Measurement plan. We will collect, analyze, and interpret data for four different alteration indices (CIA, MIA, PIA, WIS) using elemental information, primarily from SuperCam LIBS. We will initially follow the procedure laid down for ChemCam analysis by Mangold et al. (2019), i.e. excluding shots on obvious diagenetic features (based on inspection of RMI images, which are co-acquired by default for each LIBS target; Maurice et al. 2020), as well as shots for which the sum of oxide abundances is <90% (suggesting significant contamination by volatile species such as C, Cl and P to which LIBS is less sensitive). We will update these screening criteria as the mission progresses (for example, we will consider adding a carbonate correction through interpolation from PIXL/TRR/VISIR measurements of similar sites). CIA is very frequently reported and is useful for comparison purposes. The closely related Plagioclase Index of Alteration (PIA, Fedo et al. 1995) is calculated as follows: PIA = (Al_2O_3-K_2O)/(Al_2O_3+CaO*+Na_2O-K_2O). The Mafic Index of Alteration (MIA) (Babechuk et al. 2014): is calculated as follows: MIA = Al_2O_3 / (Al_2O_3 + $Fe_2O_{3(T)}$ + MgO + CaO* + Na_2O + K_2O) ×100. The MIA was developed for mafic terrains; however, the MIA has the limitation that mixed-Fe-valence minerals like magnetite cannot be accurately represented. The Weathering Index Scale (WIS) shall be calculated following the four-step protocol of

Meunier et al. 2013, assuming $Fe^{2+} \gg Fe^{3+}$ in the watershed draining into Jezero (prior to any within-the-lake oxidation). LIBS measures each of the components of the weathering indices to ±10% precision at 5 m with expected precision no worse than ChemCam (<2.1%, and typically <1%, for all these components; Maurice et al. 2020). Indeed, stratigraphic logging of the CIA has been accomplished before using ChemCam on MSL (Mangold et al. 2019). Therefore, SuperCam is a suitable tool for stratigraphic logging of CIA. According to the SuperCam team, "Shortly after landing […] compositions for SiO_2, Al_2O_3, $FeO_{(T)}$, TiO_2, CaO, MgO, Na_2O, and K_2O […] will be made available" (Maurice et al. 2020). Reported CIA errors with ChemCam at Gale are small (3-5 CIA units), and ChemCam data tracks APXS data (e.g. Mangold et al. 2019). PIXL data can be used to spot-check LIBS precision. Analysis plan. Just as on MSL (e.g. McLennan et al. 2014, Mangold et al. 2019), CIA and its variations can be interpreted in terms of changes in provenance, climate, grainsize (Siebach et al. 2017) or the extent of postdepositional open-system alteration. Just as at Gale, mineralogical information (on 2020, from SuperCam TRR/VISIR) can help to discriminate between these possibilities. For example, loss of more easily weathered minerals (e.g. olivine, pyroxenes) for constant elemental abundance would suggest that changes are not due to provenance. The protolith is largely basaltic and has been spectroscopically characterized (e.g. Goudge et al. 2015). We will consider a range of protolith compositions, using measured Mars basalt compositions (Bell et al. 2008) as well as compositions estimated from VNIR/TIR spectra of the Jezero watershed. Siliciclastic rocks on Earth have CIA values that decrease over geologic time, from ~90 in the Mesoarchean to ~72 in the Phanerozoic, and this might be the result of decreases in pCO_2 or temperature on Earth over time (González-Álvarez & Kerrich 2011). Modeling tools, for example CHIM-XPT simulations (Reed 1998, Kite & Melwani Daswani 2019), will be used to enhance the investigation by supporting interpretation of the CIA analyses (Box 1). Textural information (e.g. from PIXL) can help to diagnose source-region open system weathering versus in-place (e.g., meteoric) open system weathering (Mangold et al. 2019). Alteration index logging can also support identification of sites for sample acquisition for possible future return to Earth; isotopic data has proven decisive in tracing the timing/location of weathering during hyperthermals associated with CIA anomalies in Earth's rock record (e.g. John et al. 2012). Overall, sediment alteration index logging, in the context of the paleohydrology information from Task 1, will improve our knowledge of the relative intensity of erosion and chemical weathering (upstream and/or in-place) at Jezero, and the variations of this ratio with stratigraphic elevation. Thus it will improve our knowledge of past climate in Jezero's watershed, especially in combination with physical erosion constraints that we will obtain via Task 2.

Task 4b. Analyze element mobility in vertical profiles, e.g. late-stage wetting: Fluids for near-surface aqueous alteration on Mars were obtained from both top-down (e.g. snowmelt, lake-water infiltration), and bottom-up (groundwater) sources. Evidence for top-down alteration, forming compositionally distinct crusts, rinds, and alteration profiles is widespread on the Martian surface (e.g. Knoll et al. 2008, Arvidson et al. 2010, Ruff et al. 2014). One possible interpretation of the olivine+carbonate floor unit at Jezero is that it results from rainwater alteration of olivine-rich ash (Horgan et al. 2020). (Carbonate cementation is of particular interest because sequestration as carbonate is one possible sink for a hypothetical thick Early Mars CO_2 atmosphere). Alteration diminished over time: surface wetting $\lesssim 10^8$ yr at other landing sites is limited to surface salt precipitation and near-surface vertical transport of salts (Arvidson et al. 2010, Amundson 2018). Vertical profiles recording the length scale and magnitude of aqueous alteration can be exposed by late-stage wind erosion (Squyres et al. 2009, Williams et al. 2020), impact cratering, wheel trenching, e.t.c. Where vertical alteration profiles are suggested by color, texture (e.g. exposure surface; Stein et al. 2018), or reconnaissance elemental variations, we will plan/advocate for

LIBS profiling to constrain vertical mobilization of K, Mg, Na, and potentially other soluble elements, relative to the relatively immobile element Ti. Mobilization requires transport of ions by some aqueous fluid (McLennan & Grotzinger 2008, Hurowitz & Fischer 2014). Each of these elements are sensitive probes of past water supply and each has been previously used for this purpose at Mars (Amundson 2018, McCollom et al. 2018, Kite & Melwani Daswani 2019). The key scientific questions to be answered from analysis of these data are: which elements were most mobile, to what vertical extent where they mobile, and to what extent was their concentration enhanced or depleted? Ti normalization (e.g. Brimhall & Dietrich 1987) enables these questions to be answered using LIBS data. The paleoclimate-relevant key parameters that can be obtained from answers to these questions are: what water/rock ratio best describes the water-rock reaction, what was the direction of water flow, and (in the case of top-down alteration) what was the penetration depth of alteration (which is connected to the duration of the warm interval – seasonal or longer)? In order to relate the analyses of LIBS data to the paleoclimate-relevant key parameters, we will carry out forward models using CHIM-XPT, varying the water/rock ratio, and the paleo-pCO_2. Following Milliken et al. (2009) and Kite & Melwani Daswani (2019), we shall consider average Mars basalt and pure-olivine protolith compositions. We shall report the input parameters for each of the forward model run(s) that provide a satisfactory match to the analysis of LIBS profile data.

2.5. Work plan.

	Key Projected Milestones & Accomplishments.	Key Projected Deliverables*
Year 1	• Participate in training activities, ORT (all 3 participants). • Participate in at least 60/90 days of post-landing activities. • Document and upload all modeling tools (open-source software).	✓ Trained personnel. ✓ Contribution to daily operational roles during 60/90 days of post-landing activities.
Year 2	• Service in daily operational roles. Attendance of Team meetings. • Construct detailed plans for, target, & analyze measurements. • Detailed data analysis.	✓ LPSC presentations on Tasks 1 & 2. ✓ GRL-length paper on Task 1. ✓ GRL-length paper on Task 2.
Year3	• Service in daily operational roles. Attendance of Team meetings. • Construct detailed plans for, target, and analyze measurements. • Detailed data analysis.	✓ LPSC presentations on Tasks 3 & 4. ✓ GRL-length paper on Task 3. ✓ JGR-length paper on Task 4.
Year 4	• Close-out period. Emphasize data management and write-up. • Service in daily operational roles. Attendance of Team meetings. • Construct detailed plans for, target, and analyze measurements.	✓ JGR-length paper on Task 1 ✓ JGR-length paper on Task 2.

*We will lead-author papers as approved by the PSG, as well as provide contributions to larger Team papers as directed.

Budget analysis to ensure that participation in daily operations is sufficiently supported is included in §9.

2.6. Personnel and Qualifications. (For FTE information, see §8, Budget Justification).

The Principal Investigator (Edwin Kite) is an Assistant Professor at the University of Chicago, Kite has 14 years of experience in Early Mars research having led ~3 papers/year over the past decade on the ancient climate of Mars (both geoscience data analysis and climate / climate evolution modeling). Thus the PI is qualified to contribute to science working groups (if directed to do so by the Mars 2020 PSG), for example landing site analysis, geology and/or habitability. The PI will participate to some degree in all aspects of the proposed work and oversee its implementation. All three investigators are expected to participate in all tasks, having larger or smaller roles in each. The PI will supervise a Graduate Student Researcher at UChicago (Alexandra Warren), who will carry out part of the analysis, with emphasis on Tasks 1-2. The PI will also supervise a Postdoctoral Researcher at UChicago, who will carry out part of the analysis, with emphasis on Tasks 3-4. The PI, the postdoc, and the graduate student will each be trained to take part in daily operations and will all be available to actively and regularly take part in daily operational tasks. A letter confirming that the PI's 2.5-month FTE commitment is consistent with the PI's teaching responsibilities is included in §8 of this proposal.

3. References

R. Amundson et al. (2008), On the in situ aqueous alteration of soils on Mars, Geochimica et Cosmochimica Acta, Volume 72, Issue 15, p. 3845-3864.

R. Amundson, W. Dietrich, D. Bellugi, S. Ewing, K. Nishiizumi, G. Chong, J. Owen, R. Finkel, A. Heimsath, B. Stewart, M. Caffee, Geomorphologic evidence for the late Pliocene onset of hyperaridity in the Atacama Desert. Geol. Soc. Am. Bull. 124(7–8), 1048–1070 (2012)

R. Amundson, Meteoric water alteration of soil and landscapes at Meridiani Planum, Mars, Earth Planet. Sci. Lett., 488, p. 155-167.

J.C. Andrews-Hanna, M.T. Zuber, R.E. Arvidson, S.M. Wiseman, Early Mars hydrology: Meridiani playa deposits and the sedimentary record of Arabia Terra. J. Geophys. Res. 115(E6), E06002 (2010)

R.E. Arvidson, J.F. Bell, P. Bellutta, N.A. Cabrol, J.G. Catalano, J. Cohen, L.S. Crumpler, D.J. Des Marais, T.A. Estlin, W.H. Farrand, R. Gellert, J.A. Grant, R.N. Greenberger, E.A. Guinness, K.E. Herkenhoff, J.A. Herman, K.D. Iagnemma, J.R. Johnson, G. Klingelhöfer, R. Li, K.A. Lichtenberg, S.A. Maxwell, D.W. Ming, R.V. Morris, M.S. Rice, S.W. Ruff, A. Shaw, K.L. Siebach, A. de Souza, A.W. Stroupe, S.W. Squyres, R.J. Sullivan, K.P. Talley, J.A. Townsend, A. Wang, J.R. Wright, A.S. Yen, Spirit Mars Rover Mission: overview and selected results from the northern home plate winter haven to the side of Scamander Crater. J. Geophys. Res. 115(E12), E00F03 (2010)

M.G. Babechuk, et al., 2014, Quantifying chemical weathering intensity and trace element release from two contrasting basalt profiles, Deccan Traps, India: Chemical Geology, v.363, p. 56-75.

S.G. Banham, S. Gupta, D.M. Rubin, J.A. Watkins, D.Y. Sumner, K.S. Edgett, J.P. Grotzinger, K.W. Lewis, L.A. Edgar, K.M. Stack-Morgan, R. Barnes, J.F. Bell III, M.D. Day, R.C. Ewing, M.G.A. Lapotre, N.T. Stein, F. Rivera-Hernandez, A.R. Vasavada, Ancient Martian aeolian processes and palaeomorphology reconstructed from the Stimson formation on the lower slope of Aeolis Mons, Gale Crater, Mars. Sedimentology 65, 993–1042 (2018)

C.C. Bedford, J.C. Bridges, S.P. Schwenzer, R.C. Wiens, E.B. Rampe, J. Frydenvang, P.J. Gasda, Alteration trends and geochemical source region characteristics preserved in the fluviolacustrine sedimentary record of Gale crater, Mars. Geoch. Cosmoch. Acta 246, 234–266 (2019)

J. Bell, III (Ed.), The Martian Surface – Composition, Mineralogy, and Physical Properties. Cambridge University Press, pp. 519–540

E.K. Berner and R. A. Berner, 2012, Global Environment: Water, Air, and Geochemical Cycles, Princeton University Press.

J.L. Bishop, AG Fairén, JR Michalski, L Gago-Duport, LL Baker, MA Velbel, et al., 2018, Surface clay formation during short-term warmer and wetter conditions on a largely cold ancient Mars, Nature Astronomy 2 (3), 206-213

G.H. Brimhall, & W. E. Dietrich, 1987, Constitutive mass balance relations between chemical composition, volume, density, porosity, and strain in metasomatic hydrochemical systems: Results on weathering and pedogenesis, 51(3), 567-587.

T.F. Bristow, E.B. Rampe, C.N. Achilles, D.F. Blake, S.J. Chipera, P. Craig, J.A. Crisp, D.J. Des Marais et al., Clay mineral diversity and abundance in sedimentary rocks of Gale Crater, Mars. Sci. Adv. 4(6), eaar3330 (2018). https://doi.org/10.1126/sciadv.aar3330

A. J. Brown C. E. Viviano T. A. Goudge, 2020, Olivine-Carbonate Mineralogy of the Jezero Crater Region, Icarus https://doi.org/10.1029/2019JE006011

M.A. Bullock & J. M. Moore, 2007, Atmospheric conditions on early Mars and the missing layered carbonates, Geophysical Research Letters Volume 34, Issue 19.

D. M. Burr, R. M. E. Williams, K. D. Wendell, M. Chojnacki, J. P. Emery, Inverted fluvial features in the Aeolis/Zephyria plana region, Mars: Formation mechanism and initial paleodischarge estimates. J. Geophys. Res. 115, E07011 (2010)

D. Buscombe, 2008, Estimation of grain-size distributions and associated parameters from digital images of sediment, Sedimentary Geology 210, 1-10.

M.H. Carr, The Surface of Mars (Cambridge University Press, Cambridge, 2006)

S Carretier, V Regard, L Leanni, M Farias, 2019, Long-term dispersion of river gravel in a canyon in the Atacama Desert, Central Andes, deduced from their 10 Be concentrations, Scientific reports 9 (1), 1-12

J. Carter et al. 2015 Orbital detection and implications of akaganéite on Mars Icarus Volume 253, June 2015, Pages 296-310

D.C. Catling, J.F. Kasting, Atmospheric Evolution on Inhabited and Lifeless Worlds (Cambridge University Press, Cambridge, 2017)

D. C. Catling & K. J. Zahnle. The Archean Atmosphere, Science Advances 6, eaax1420, 2020, doi: 10.1126/sciadv.aax1420

S. M. Chemtob et al. 2017, Oxidative Alteration of Ferrous Smectites and Implications for the Redox Evolution of Early Mars, Journal of Geophysical Research: PlanetsVolume 122, Issue 12

Barbara A. Cohen, Charles A. Malespin, Kenneth A. Farley, Peter E. Martin, Yuichiro Cho, and Paul R. Mahaffy, 2019, In Situ Geochronology on Mars and the Development of Future Instrumentation, Astrobiology, Vol. 19, No. 11, https://doi.org/10.1089/ast.2018.1871.

R.A. DiBiase, A.B. Limaye, J.S. Scheingross, W.W. Fischer, M.P. Lamb, Deltaic deposits at Aeolis Dorsa: sedimentary evidence for a standing body of water on the northern plains of Mars. J. Geophys. Res., Planets 118(6), 1285–1302 (2013)

W.E. Dietrich, M.C. Palucis, R.M.E. Williams, K.W. Lewis, F. Rivera-Hernandez, D.Y. Sumner, Fluvial gravels on Mars: analysis and implications, in Gravel Bed Rivers: Processes and Disasters, ed. by D. Tsutsumi, J.B. Laronne (Wiley, New York, 2017), pp. 755–783

J. Drever 1997 The Geochemistry of Natural Waters: Surface and Groundwater Environments (3rd Edition) 3rd Edition, Prentice Hall.

M. Dundar, B. Ehlmann, and E. Leask, 2019, Machine-Learning-Driven New Geologic Discoveries at Mars Rover Landing Sites: Jezero and NE Syrtis, arXiv:1909.02387

C.M. Dundas, L.P. Keszthelyi, V.J. Bray, A.S. McEwen, Role of material properties in the cratering record of young platy-ridged lava on Mars, Geophys. Res. Lett., 37 (2010), p. L12203

B.C. Eaton, Chap. 9.18: hydraulic geometry, in Treatise on Geomorphology, 9, Fluvial Geomorphology, ed. by E.E. Wohl (Elsevier, Oxford, 2013)

K.S. Edgett, M.C. Malin, Martian sedimentary rock stratigraphy: outcrops and interbedded craters of northwest Sinus Meridiani and southwest Arabia Terra. Geophys. Res. Lett. 29(24), 2179 (2002). https:// doi.org/10.1029/2002GL016515

J. Eigenbrode et al. 2018, Organic matter preserved in 3-billion-year-old mudstones at Gale crater, Mars, Science, Volume 360, Issue 6393, pp. 1096-1101.

B.L. Ehlmann, J.F. Mustard, S.L. Murchie et al., Subsurface water and clay mineral formation during the early history of Mars. Nature 479(7371), 53–60 (2011a)

B.L. Ehlmann, F.S. Anderson, J. Andrews-Hanna, D.C. Catling, R. Christensen, B.A. Cohen, C.D. Dressing, C.S. Edwards, L.T. Elkins-Tanton, K.A. Farley, C.I. Fassett, W.W. Fischer, A.A. Fraeman, M.P. Golombek, V.E. Hamilton, A.G. Hayes, C.D.K. Herd, B. Horgan, R. Hu, B.M. Jakosky, J.R. Johnson, J.F. Kasting, L. Kerber, K.M. Kinch, E.S. Kite, H.A. Knutson, J.I. Lunine, R. Mahaffy, N. Mangold, F.M. McCubbin, J.F. Mustard, B. Niles, C. Quantin-Nataf, M.S. Rice, K.M. Stack, D.J. Stevenson, S.T. Stewart, M.J. Toplis, T. Usui, B.P. Weiss, S.C. Werner, R.D. Wordsworth, J.J. Wray, R.A. Yingst, Y.L. Yung, K.J. Zahnle, The sustainability of habitability on terrestrial planets: insights, questions, and needed measurements from Mars for understanding the evolution of Earth-like worlds. J. Geophys. Res., Planets 121(10), 1927–1961 (2016)

M.E. Elwood Madden, A.S. Madden, J.D. Rimstidt, How long was Meridiani Planum wet? Applying a jarosite stopwatch to determine the duration of aqueous diagenesis. Geology 37(7), 635–638 (2009)

A.G. Fairén, Alfonso F. Davila, Luis Gago-Duport, Jacob D. Haqq-Misra, Carolina Gil, Christopher P. McKay & James F. Kasting, 2011, Cold glacial oceans would have inhibited phyllosilicate sedimentation on early Mars, Nature Geoscience volume 4, 667–670.

K.A. Farley, C. Malespin, P. Mahaffy, J.P. Grotzinger, P.M. Vasconcelos, R.E. Milliken, M. Malin, K.S. Edgett, A.A. Pavlov, J.A. Hurowitz, J.A. Grant et al., In situ radiometric and exposure age dating of the Martian surface. Science 343(6169), 1247166 (2014

C.I. Fassett, J.W. Head, Fluvial sedimentary deposits on Mars: ancient deltas in a crater lake in the Nili Fossae region. Geophys. Res. Lett. 32(14), L14201 (2005)

C.I. Fassett, J.W. Head, The timing of Martian valley network activity: constraints from buffered crater counting. Icarus 195(1), 61–89 (2008a)

C. Fedo, H.W. Nesbitt, G.M. Young, Unraveling the effects of potassium metasomatism in sedimentary rocks and paleosols, with implications for paleoweathering conditions and provenance, Geology, 23 (1995), pp. 921-924.

C.M. Fedo, J.P. Grotzinger, S. Gupta, N.T. Stein, J. Watkins, S. Banham, K.S. Edgett, M. Minitti, J. Schieber, K. Siebach, K. Stack-Morgan, H. Newsom, K.W. Lewis, C. House, A.R. Vasavada, Facies analysis and basin architecture of the upper part of the Murray formation, Gale Crater, Mars, in 48th Lunar and Planetary Science Conference. 20–24 March 2017, The Woodlands, Texas. LPI Contribution, vol. 1964 (2017), p. 1689

B.Z. Foreman, et al. (2012), Fluvial response to abrupt global warming at the Palaeocene/Eocene boundary. Nature, 491, 92-95.

H. Franz et al. 2020, Indigenous and exogenous organics and surface-atmosphere cycling inferred from carbon and oxygen isotopes at Gale crater, Nature Astronomy, Advanced Online Publication, doi: 10.1038/s41550-019-0990-x

L.R. Gabasova, E.S. Kite, Compaction and sedimentary basin analysis on Mars. Planet. Space Sci. 152, 86– 106 (2018)

M.P. Golombek, N.H. Warner, V. Ganti, M.P. Lamb, T.J. Parker, R.L. Fergason, R. Sullivan, Small crater modification on Meridiani Planum and implications for erosion rates and climate change on Mars. J. Geophys. Res., Planets 119(12), 2522–2547 (2014)

I. González-Álvarez, R Kerrich, 2012, Weathering intensity in the Mesoproterozoic and modern large-river systems: A comparative study in the Belt-Purcell Supergroup, Canada and USA Precambrian Research, 208, 174.

T. A., Goudge, J. F. Mustard, J. W. Head, C. I. Fassett, and S. M. Wiseman (2015), Assessing the mineralogy of the watershed and fan deposits of the Jezero crater paleolake system, Mars, J. Geophys. Res., 120, 775–808.

T.A. Goudge, R.E. Milliken, J.W. Head, J.F. Mustard, C.I. Fassett, Sedimentological evidence for a deltaic origin of the western fan deposit in Jezero Crater, Mars and implications for future exploration. Earth Planet. Sci. Lett. 458, 357–365 (2017)

T.A. Goudge, D. Mohrig, B.T. Cardenas, C.M. Hughes, C.I. Fassett, Stratigraphy and paleohydrology of delta channel deposits, Jezero Crater, Mars. Icarus 301, 58–75 (2018)

PM Grindrod, NH Warner, Erosion rate and previous extent of interior layered deposits on Mars revealed by obstructed landslides, Geology 42 (9), 795-798

J. Grotzinger et al. 2011, Mars sedimentary geology: key concepts and outstanding questions, Astrobiology, Jan. 2011, 77-87.

J.P. Grotzinger, D.Y. Sumner, L.C. Kah, K. Stack, S. Gupta, L. Edgar, D. Rubin, K. Lewis, J. Schieber, N. Mangold, R. Milliken, G. Conrad, D. DesMarais, J. Farmer, K. Siebach, F. Calef, J. Hurowitz, S.M. McLennan et al., A Habitable Fluvio-Lacustrine environment at Yellowknife bay, Gale Crater, Mars. Science 343(6169), 1242777 (2014)

J. Grotzinger et al. 2015, Deposition, exhumation, and paleoclimate of an ancient lake deposit, Gale crater, Mars, Vol. 350, Issue 6257, aac7575.

R.M. Haberle, Early Mars climate models. J. Geophys. Res. 103(E12), 28467–28480 (1998)

R.M. Haberle, D.C. Catling, M.H. Carr, K.J. Zahnle, The early Mars climate system, in The Atmosphere and Climate of Mars, ed. by R.M. Haberle et al.(Cambridge University Press, Cambridge, 2017), pp. 497–525. ISBN 9781139060172

I. Halevy & D. Schrag, 2009, Sulfur dioxide inhibits calcium carbonate precipitation: Implications for early Mars and Earth, Geophys. Res. Lett. 36(23).

J. Hao et al. 2017, A model for late Archean chemical weathering and world average river water, Earth & Planet. Sci. Lett. 457, 191-203.

I. Halevy, J.W. Head III, Episodic warming of early Mars by punctuated volcanism. Nat. Geosci. 7(12), 865–868 (2014)

V.E. Hamilton & P. Christensen 2005, Evidence for extensive, olivine-rich bedrock on Mars, Geology (2005) 33 (6): 433–436.

E. Hajek & P. Heller 2012, Flow-Depth Scaling In Alluvial Architecture and Nonmarine Sequence Stratigraphy: Example from the Castlegate Sandstone, Central Utah, U.S.A, Journal of Sedimentary Research (2012) 82 (2): 121–130.

E.A., Hajek, & Wolinsky, M.A. (2012), Simplified process modeling of river avulsion and alluvial architecture: Connecting models and field data, Sedimentary Geology, 257-260, 1-30.

W. Hartmann, 2005, Martian cratering 8: Isochron refinement and the chronology of Mars, Icarus, Volume 174, Issue 2, April 2005, Pages 294-320.

E.M. Hausrath, A.K. Navarre-Sitchler, P.B. Sak et al., Basalt weathering rates on Earth and the duration of liquid water on the plains of Gusev Crater, Mars. Geology 36(1), 67–70 (2008)

A.T. Hayden et al. 2019, Formation of sinuous ridges by inversion of river-channel belts in Utah, USA, with implications for Mars, Volume 332, 1 November 2019, Pages 92-110.

A.M. Hessler et al. 2004, A lower limit for atmospheric carbon dioxide levels 3.2 billion years ago, Nature volume 428, pages736–738.

H. Holland 1984, The Chemical Evolution of the Atmosphere and Oceans, Princeton University Press.

B. Horgan et al. 2020, The mineral diversity of Jezero crater: Evidence for possible lacustrine carbonates on Mars, Volume 339, 15 March 2020, 113526

A.D. Howard, A.T. Hemberger, 1991, Multivariate characterization of meandering Geomorphology, 4 (1991), pp. 161-186

J.A. Hurowitz, S.M. McLennan, A ~ 3.5 Ga record of water-limited, acidic weathering conditions on Mars. Earth Planet. Sci. Lett. 260(3–4), 432–443 (2007)

J.A. Hurowitz, W.W. Fischer, Contrasting styles of water-rock interaction at the Mars Exploration Rover landing sites. Geochim. Cosmochim. Acta 127, 25–38 (2014)

J.A. Hurowitz, J.P. Grotzinger, W.W. Fischer, S.M. McLennan, R.E. Milliken, N. Stein, A.R. Vasavada, D.F. Blake, E. Dehouck, J.L. Eigenbrode, A.G. Fairén, J. Frydenvang, R. Gellert, J.A. Grant, S. Gupta, K.E. Herkenhoff, D.W. Ming, E.B. Rampe, M.E. Schmidt, K.L. Siebach, K. Stack-Morgan, D.Y. Sumner, R.C. Wiens, Redox stratification of an ancient lake in Gale Crater, Mars. Science 356(6341), aah6849 (2017)

P. Huybers & W. Curry 2006, Links between annual, Milankovitch and continuum temperature variability, Nature 441, pages 329–332.

R.P. Irwin, A.D. Howard, R.A. Craddock, J.M. Moore, An intense terminal epoch of widespread fluvial activity on early Mars: 2. Increased runoff and paleolake development. J. Geophys. Res. 110(E12), E12S15 (2005a)

R.P. Irwin, K.W. Lewis, A.D. Howard, J.A. Grant, Paleohydrology of Eberswalde crater, Mars. Geomorphology (2015). https://doi.org/10.1016/j.geomorph.2014.10.012

C. M. John et al., 2012, Clay assemblage and oxygen isotopic constraints on the weathering response to the Paleocene-Eocene thermal maximum, east coast of North America , Geology (2012) 40 (7): 591–594.

J.E. Johnson et al. 2014, O_2 constraints from Paleoproterozoic detrital pyrite and uraninite, GSA Bulletin (2014) 126 (5-6): 813–830.

E.S. Kite, I. Halevy, M.A. Kahre, M.J. Wolff, M. Manga, Seasonal melting and the formation of sedimentary rocks on Mars, with predictions for the Gale Crater mound. Icarus 223(1), 181–210 (2013a)

E.S. Kite, A. Lucas, C.I. Fassett, Pacing Early Mars river activity: embedded craters in the Aeolis Dorsa region imply river activity spanned (1–20) Myr. Icarus 225, 850–855 (2013b)

E.S. Kite, J.-P. Williams, A. Lucas, O. Aharonson, Low palaeopressure of the Martian atmosphere estimated from the size distribution of ancient craters. Nat. Geosci. 7(5), 335–339 (2014)

E.S. Kite, Howard, A., Lucas, A., & Lewis, K.W., 2015a. Resolving the era of river-forming climates on Mars using stratigraphic logs of river-deposit dimensions, Earth & Planetary Science Letters, 420, 55-65, doi:10.1016/j.epsl.2015.03.019

E.S. Kite, A.D. Howard, A.S. Lucas, J.C. Armstrong, O. Aharonson, M.P. Lamb, Stratigraphy of Aeolis Dorsa, Mars: stratigraphic context of the great river deposits. Icarus 253, 223–242 (2015b)

E.S. Kite, Sneed, J., Mayer, D.P., Lewis, K.W., Michaels, T.I., Hore, A., & Rafkin, S.C.R., 2016. Evolution of major sedimentary mounds on Mars, Journal of Geophysical Research – Planets, 121, 2282-2324.

E.S. Kite, P. Gao, C. Goldblatt, M.A. Mischna, D.P. Mayer, Y.L. Yung, Methane bursts as a trigger for intermittent lake-forming climates on post-Noachian Mars. Nat. Geosci. 10, 737–740 (2017a)

E.S. Kite, J. Sneed, D.P. Mayer, S.A. Wilson, Persistent or repeated surface habitability on Mars during the late Hesperian–Amazonian. Geophys. Res. Lett. 44(9), 3991–3999 (2017b)

E.S. Kite, & Mayer, D.P., 2017. "Mars sedimentary rock erosion rates constrained using crater counts, with applications to organic-matter preservation and to the global dust cycle," Icarus, 286, 212-222, doi:10.1016/j.icarus.2016.10.010.

E.S. Kite, & Ford, E., 2018, "Habitability of exoplanet waterworlds," Astrophysical Journal, 864, 75, 28 pp, doi.org/10.3847/1538-4357/aad6e0.

E.S. Kite, L.J. Steele, M.A. Mischna, The cirrus cloud greenhouse on Early Mars: an explanation, the explanation, or no explanation for rivers and lakes? in AGU Fall Meeting (2018), P51F-2942

E.S. Kite, D.P. Mayer, S.A. Wilson, J.M. Davis, A.S. Lucas, G. Stucky de Quay, Persistence of intense, climate-driven runoff late in Mars history. Sci. Adv. (2019, in press)

E.S. Kite, 2019, "Geologic constraints on Early Mars climate," Space Science Reviews, 215: 10, doi:10.1007/s11214-018-0575-5.

E.S. Kite, & Melwani Daswani, M., 2019, "Geochemistry constrains global hydrology on Early Mars," Earth & Planetary Science Letters, 524, 115718, 10 pp.

E.S. Kite, Steele, L., and Mischna, M., 2019, Aridity enables warm climates on Mars, LPSC, https://www.hou.usra.edu/meetings/lpsc2019/pdf/1360.pdf

M.G. Kleinhans, Flow discharge and sediment transport models for estimating a minimum timescale of hydrological activity and channel and delta formation on Mars. J. Geophys. Res. 110(E12), E12003 (2005)

M.G. Kleinhans, H.E. van de Kasteele, E. Hauber, Palaeoflow reconstruction from fan delta morphology on Mars. Earth Planet. Sci. Lett. 294(3–4), 378–392 (2010)

Knoll, A.H. et al., 2008. Veneers, rinds, and fracture fills: Relatively late alteration of sedimentary rocks at Meridiani Planum, Mars. J. Geophys. Res. 113, E06S16.

G. Kondolf 1997, APPLICATION OF THE PEBBLE COUNT: NOTES ON PURPOSE, METHOD, AND VARIANTS, J. American Water Resources Association 33(1).

N. Lanza et al. 2016, Oxidation of manganese in an ancient aquifer, Kimberley formation, Gale crater, Mars, Geophys. Res. Lett. 43(14).

M. Lapotre & A. Ielpi 2019, P54C-08 - The western delta deposits of Jezero crater, Mars, as a quantitative paleoclimatic record: Timescales and intermittency of surface flows on Early Mars, AGU Fall Meeting.

S.F. Leclair and J. Bridge, Quantitative Interpretation of Sedimentary Structures Formed by River Dunes, Journal of Sedimentary Research (2001) 71 (5): 713–716.

A. Lefort, D.M. Burr, R.A. Beyer, A.D. Howard, Inverted fluvial features in the Aeolis-Zephyria plana, western Medusae Fossae formation, Mars: evidence for post-formation modification. J. Geophys. Res. 117(E3), E03007 (2012)

K.W. Lewis, and O. Aharonson (2014), Occurrence and origin of rhythmic sedimentary rocks on Mars, J. Geophys. Res. Planets, 119, 1432–1457, doi:10.1002/2013JE004404.

H. Ma et al., 2017, The exceptional sediment load of fine-grained dispersal systems: Example of the Yellow River, China, Science Advances 12 May 2017: Vol. 3, no. 5, e1603114, DOI: 10.1126/sciadv.1603114

H Ma, JA Nittrouer, B Wu, MP Lamb, Y Zhang, D Mohrig, X Fu, K Naito, 2020, Universal relation with regime transition for sediment transport in fine-grained rivers, Proceedings of the National Academy of Sciences 117 (1), 171-176

M.C. Malin, K.S. Edgett, B.A. Cantor, M.A. Caplinger, G.E. Danielson, E.H. Jensen, M.A. Ravine, J.L. Sandoval, K.D. Supulver, An overview of the 1985–2006 Mars orbiter camera science investigation. Mars Int. J. Mars Sci. Explor. 4, 1–60 (2010)

L. Mandon et al. 2020, Refining the age, emplacement and alteration scenarios of the olivine-rich unit in the Nili Fossae region, Mars, Icarus, Volume 336, 15 January 2020, 113436.

N. Mangold, Kite, E.S., Kleinhans, M., Newsom, H.E., Ansan, V., Hauber, E., Kraal, E., Quantin-Nataf, C. & K. Tanaka, 2012. "The origin and timing of fluvial activity at Eberswalde Crater, Mars," Icarus, 220, 530-551, doi:10.1016/j.icarus.2012.05.026.

N. Mangold et al. 2016, Composition of conglomerates analyzed by the Curiosity rover: Implications for Gale Crater crust and sediment sources, J. Geophys. Res. Planets, 121, 353–387, doi:10.1002/2015JE004977.

N. Mangold, G. Dromart, F. Salese, V. Ansan, and M. Massé, 2018, Constraints on the duration of fluvial and lacustrine activity at Jezero crater, presentation at Mars 2020 Fourth Landing Site Workshop, presentation available at https://marsnext.jpl.nasa.gov/workshops/wkshp_2018_10.cfm

N. Mangold et al., Chemical alteration of fine-grained sedimentary rocks at Gale crater. Icarus 321, 619–631 (2019)

P.E. Marcelo Garcia, Sedimentation Engineering: Processes, Measurements, Modeling, and Practice. MOP, vol. 110 (American Society of Civil Engineers, Reston, 2008). ISBN 978-0-7844-0814-8

Mars 2020 Landing Site Working Group (2018), Jezero Operations Scenarios, presentation at Mars 2020 Fourth Landing Site Workshop, presentation available at https://marsnext.jpl.nasa.gov/workshops/wkshp_2018_10.cfm (250 MB file)

S. Maurice et al. 2020, Mars 2020 SuperCam Webinar (official SuperCam team presentation, publicly available and linked from NSPIRES FAQ for the Announcement of Opportunity for this Participating Scientist call); all webinar information including slides available at https://pds-geosciences.wustl.edu/workshops/SuperCam _Workshop_Feb2020.htm

McCollom, T.M., 2018. Geochemical trends in the Burns formation layered sulfate deposits at Meridiani Planum, Mars, and implications for their origin. J. Geophys. Res., Planets 123, 2393–2429.

S.M. McLennan, R.B. Anderson, J.F. Bell III et al., Elemental geochemistry of sedimentary rocks at Yellowknife bay, Gale Crater, Mars. Science 343(6169), 1244734

S.M. McLennan, J.P. Grotzinger, J.A. Hurowitz, N.J. Tosca, The sedimentary cycle on Early Mars. Annu. Rev. Earth Planet. Sci. 47 (2019).

MEPAG, 2018, Mars Scientific Goals, Objectives, Investigations, and Priorities: 2018. D. Banfield, ed., 81 p. white paper posted October, 2018 by the Mars Exploration Program Analysis Group (MEPAG) at https://mepag.jpl.nasa.gov/reports.cfm

J.M. Metz, J.P. Grotzinger, D.M. Rubin, K.W. Lewis, S.W. Squyres, J.F. Bell, Sulfate-rich Eolian and wet interdune deposits, Erebus Crater, Mars. J. Sediment. Res. 79, 247–264 (2009)

C.P. McKay, D.T. Andersen, W.H. Pollard, J.L. Heldmann, P.T. Doran, C.H. Fritsen, J.C. Priscu, Polar lakes, streams, and springs as analogs for the hydrological cycle on Mars, in Water on Mars and Life (Springer, Berlin, 2005), pp. 219–233

S.M. McLennan, J.P. Grotzinger, The sedimentary rock cycle of Mars, in The Martian Surface—Composition, Mineralogy, and Physical Properties, ed. by J Bell III (Cambridge University Press, Cambridge, 2008), p. 541. ISBN 9780521866989

S.M. McLennan, Geochemistry of sedimentary processes on Mars, in Sedimentary Geology of Mars, ed. by Grotzinger, Milliken. SEPM Special Publication, vol. 102 (SEPM, McLean, 2012), pp. 119–138. ISBN 978-1-56576-312-8

S.M. McLennan, et al. Elemental geochemistry of sedimentary rocks in Yellowknife Bay, Gale Crater, Mars, Science, 343 (2014), 10.1126/science.1244734

A. Meunier et al. 2013, The weathering intensity scale (WIS): An alternative approach of the Chemical Index of Alteration (CIA), Am. J. Sci., February 2013 vol. 313 no. 2 113-143.

G.G. Michael, Planetary surface dating from crater size-frequency distribution measurements: multiple resurfacing episodes and differential isochron fitting. Icarus 226(1), 885–890 (2013)

D Mohrig, PL Heller, C Paola, WJ Lyons, 2000, Interpreting avulsion process from ancient alluvial sequences: Guadalope-Matarranya system (northern Spain) and Wasatch Formation (western Colorado), Geological Society of America Bulletin 112 (12), 1787-1803.

J.J. Moore, K.A. Hughen, G.H. Miller & J.T. Overpeck, 2001, Little Ice Age recorded in summer temperature reconstruction from vared sediments of Donard Lake, Baffin Island, Canada, Journal of Paleolimnology volume 25, pages503–517(2001)

J.W. Morse & R.S. Arvidson 2002, The dissolution kinetics of major sedimentary carbonate minerals, Earth-Science Reviews, Volume 58, Issues 1–2, July 2002, Pages 51-84

H.W. Nesbitt & G.M. Young 1982, Early Proterozoic climates and plate motions inferred from major element chemistry of lutites, Nature 299, 715

A. Ody et al. 2013, Global investigation of olivine on Mars: Insights into crust and mantle compositions, J. Geophys. Res., Volume118, Pages 234-262

A.A. Olson, J.D. Rimstidt, Using a mineral lifetime diagram to evaluate the persistence of olivine on Mars. Am. Mineral. 92(4), 598–602 (2007)

P. Olsen et al. 2019, Mapping Solar System chaos with the Geological Orrery, PNAS May 28, 2019 116 (22) 10664-10673.

Palandri & Kharaka 2004, A Compilation of Rate Parameters of Water-Mineral Interaction Kinetics for Application to Geochemical Modeling, USGS Open File Report, https://pubs.usgs.gov/of/2004/1068/

A. Palumbo & J. Head 2018, Early Mars Climate History: Characterizing a "Warm and Wet" Martian Climate With a 3‐D Global Climate Model and Testing Geological Predictions, Geophys. Res. Lett 45(19), https://doi.org/10.1029/2018GL079767

M.C. Palucis, W.E. Dietrich, R.M.E. Williams, A.G. Hayes, T. Parker, D.Y. Sumner, N. Mangold, K. Lewis, H. Newsom, Sequence and relative timing of large lakes in Gale Crater (Mars) after the formation of Mount Sharp. J. Geophys. Res., Planets 121(3), 472–496 (2016)

G. Parker, P. Wilcock, C. Paola, W.E. Dietrich, J. Pitlick, Physical basis for quasi-universal relations describing bankfull hydraulic geometry of single-thread gravel bed rivers. J. Geophys. Res., Earth Surf. 112(F4), F04005 (2007)

A.M. Pfeiffer, N.J. Finnegan, J.K. Willenbring, Sediment supply controls equilibrium channel geometry in gravel rivers. Proc. Natl. Acad. Sci. 114(13), 3346–3351 (2017)

O.S. Pokrovsky et al., 2009, Calcite, dolomite and magnesite dissolution kinetics in aqueous solutions at acid to circumneutral pH, 25 to 150 °C and 1 to 55 atm pCO2: New constraints on CO2 sequestration in sedimentary basins, Volume 265, Issues 1–2, 15 July 2009, Pages 20-32.

R.M. Ramirez, A warmer and wetter solution for early Mars and the challenges with transient warming. Icarus 297, 71–82 (2017)

B. Rasmussen & R. Buick 1999, Redox state of the Archean atmosphere: Evidence from detrital heavy minerals in ca. 3250 2750 Ma sandstones from the Pilbara Craton, Australia, Geology, vol. 27, Issue 2, p.115

W. Rapin, et al. 2019 An interval of high salinity in ancient Gale crater lake on Mars, Nature Geoscience, Volume 12, Issue 11, p.889-895

M. H. Reed, (1998), Calculation of simultaneous chemical equilibria in aqueous-mineral-gas systems and its application to modeling hydrothermal processes, in Techniques in Hydrothermal Ore Deposits Geology, Reviews in Economic Geology, vol. 10, edited by J. P. Richards and P. B. Larson, pp. 109–124, Society of Economic Geologists, Littleton, Colorado.

M. Ren, & Shi. Y.-L., 1986, Sediment discharge of the Yellow River (China) and its effect on the sedimentation of the Bohai and the Yellow Sea, Continental Shelf-Research, 6, 785-810.

M. Richardson et al. (2007), PlanetWRF: A general purpose, local to global numerical model for planetary atmospheric and climate dynamics, J. Geophys. Res., 112(E9).

F. Rivera-Hernández et al. (2019), Using ChemCam LIBS data to constrain grain size in rocks on Mars: Proof of concept and application to rocks at Yellowknife Bay and Pahrump Hills, Gale crater, Icarus 321, 82-98.

D. Rubin et al. 2015 Sedimentary Facies as Indicators of Changing Lake Levels in Gale Crater, Mars, American Geophysical Union, Fall Meeting 2015, abstract id.P43B-2116

S.W. Ruff, P.B. Niles, F. Alfano, A.B. Clarke, Evidence for a Noachian-aged ephemeral lake in Gusev Crater, Mars. Geology 42(4), 359–362 (2014)

S.W. Ruff, V.E. Hamilton, Wishstone to watchtower: amorphous alteration of plagioclase-rich rocks in Gusev Crater, Mars. Am. Mineral. 102(2), 235–251 (2017)

C. Sagan, O.B. Toon, P. Gierasch, 1973, Climatic change on Mars, Science, 181 (1973), pp. 1045-1049.

F Salese, N Mangold, MG Kleinhans, T de Haas, V Ansan, G Dromart, 2019 Estimated Minimum Lifespan of the Jezero Crater Delta, Mars, LPSC, https://www.hou.usra.edu/meetings/lpsc2019/pdf/2107.pdf

S. Schon et al. 2012 An overfilled lacustrine system and progradational delta in Jezero crater, Mars: Implications for Noachian climate, Planetary and Space Science Volume 67, Issue 1, July 2012, Pages 28-45.

J. Schieber et al. 2017, Encounters with an unearthly mudstone: Understanding the first mudstone found on Mars, Sedimentology 64 (2), 311-358

Shao, Y., 2008, Physics and modeling of wind erosion, 2nd revised and expanded edition, Springer.

S. Sharhzad et al., 2019, Crater Statistics on the Dark‐Toned, Mafic Floor Unit in Jezero Crater, Mars, Geophys. Res. Lett., https://doi.org/10.1029/2018GL081402.

K.L. Siebach, M.B. Baker, J.P. Grotzinger, S.M. McLennan, R. Gellert, L.M. Thompson, J.A. Hurowitz, Sorting out compositional trends in sedimentary rocks of the Bradbury group (Aeolis Palus), Gale Crater, Mars. J. Geophys. Res., Planets 122(2), 295–328 (2017)

HD Sinclair, FM Stuart, SM Mudd, L McCann, Z Tao, 2019, Detrital cosmogenic 21Ne records decoupling of source-to-sink signals by sediment storage and recycling in Miocene to present rivers of the Great Plains, Nebraska, USA, Geology 47 (1), 3-6.

S. Squyres, S. W., 1989, Urey prize lecture - Water on Mars, Icarus (ISSN 0019-1035), 79, June 1989, p. 229-288.

S.W. Squyres, R.E. Arvidson, D.L. Blaney, B.C. Clark, L. Crumpler, W.H. Farrand, S. Gorevan, K.E. Herkenhoff, J. Hurowitz, A. Kusack, H.Y. McSween, D.W. Ming, R.V. Morris, S.W. Ruff, A. Wang, A. Yen, Rocks of the Columbia Hills. J. Geophys. Res. 111, E2, E02S11 (2006)

S. Squyres, S., et al. 2009, Exploration of Victoria Crater by the Mars Rover Opportunity, Science 22 May 2009: Vol. 324, Issue 5930, pp. 1058-1061.

K. Stack et al. 2013, Bed thickness distributions on Mars: An orbital perspective, J. Geophys. Res. 118(6), https://doi.org/10.1002/jgre.20092

K.E. Steakley, M.A. Kahre, J.R. Murphy, R.M. Haberle, A. Kling, Revisiting the impact heating hypothesis for early Mars with a 3D GCM, in Fourth International Conference on Early Mars, Proceedings of the Conference, 2–6 October, 2017, Flagstaff, Arizona. LPI Contribution, vol. 2014 (2017), p. 3074

J.D. Stopar, G.J. Taylor, V.E. Hamilton, L. Browning, Kinetic model of olivine dissolution and extent of aqueous alteration on Mars. Geochim. Cosmochim. Acta 70(24), 6136–6152 (2006)

N. Stein, J.P. Grotzinger, J. Schieber, N. Mangold, B. Hallet, H. Newsom, K.M. Stack, J.A. Berger, L. Thompson, K.L. Siebach, A. Cousin, S. Le Mouélic, M. Minitti, D.Y. Sumner, C. Fedo, C.H. House, S. Gupta, A.R. Vasavada, R. Gellert, R.C. Wiens, J. Frydenvang, O. Forni, P.Y.M.V. Payré, E. Dehouck, Desiccation cracks provide evidence of lake drying on Mars, Sutton Island member, Murray formation, Gale Crater. Geology 46(6), 515–518 (2018)

T. Szabó, Gábor Domokos, John P. Grotzinger & Douglas J. Jerolmack, 2015, Reconstructing the transport history of pebbles on Mars, Nature Communications volume 6, Article number: 8366.

JD Tarnas, JF Mustard, H Lin, TA Goudge, ES Amador, MS Bramble, 2019, Orbital identification of hydrated silica in Jezero crater, Mars, Geophysical Research Letters 46 (22), 12771-12782

N.J. Tosca, A.H. Knoll, Juvenile chemical sediments and the long term persistence of water at the surface of Mars. Earth Planet. Sci. Lett. 286(3–4), 379–386 (2009)

N.J. Tosca, I.A.M. Ahmed, B.M. Tutolo, A. Ashpitel, J.A. Hurowitz, Magnetite authigenesis and the warming of early Mars. Nat. Geosci. 11, 635–639 (2018)

M. Turbet et al., 2019, Far infrared measurements of absorptions by $CH_4 + CO_2$ and $H_2 + CO_2$ mixtures and implications for greenhouse warming on early Mars, Icarus 321, 189-199.

M. Turbet, C. Boulet & T. Karman, 2020a, Measurements and parameterizations of CO2+CH4 and CO_2+H_2 collision-induced absorptions across a wide range of wavenumbers and temperatures. Application for the prediction of early Mars surface temperature, arXiv:1912.05630.

M. Turbet, C. Gillmann, B. Baudin, F. Forget, A. Palumbo, J.W. Head & O. Karatekin, The environmental effects of very large bolide impacts on early Mars explored with a hierarchy of numerical models, Icarus, 2020b.

A.R. Vasavada, Our changing view of Mars. Phys. Today 70(3), 34–41 (2017)

A. Wang, L.A. Haskin, S.W. Squyres, B.L. Jolliff, L. Crumpler, R. Gellert, C. Schröder, K. Herkenhoff, J. Hurowitz, N.J. Tosca, W.H. Farrand, R. Anderson, A.T. Knudson, Sulfate deposition in subsurface regolith in Gusev Crater, Mars. J. Geophys. Res. 111, E2, E02S17 (2006)

P. Ward et al. 2000 Altered River Morphology in South Africa Related to the Permian-Triassic Extinction, Science, Volume 289, Issue 5485, pp. 1740-1743 (2000).

A.O. Warren, E.S. Kite, et al. 2019, Through the Thick and Thin: New Constraints on Mars Paleopressure History 3.8 - 4 Ga from Small Exhumed Craters, Journal of Geophysical Research: Planets, Volume 124, Issue 11, pp. 2793-2818.

R.M.E. Williams, J.P. Grotzinger, W.E. Dietrich, S. Gupta, D.Y. Sumner, R.C. Wiens, N. Mangold, M.C. Malin, K.S. Edgett et al., Martian fluvial conglomerates at Gale Crater. Science 340(6136), 1068–1072 (2013)

R.M.E. Williams & C. Weitz 2014, Reconstructing the aqueous history within the southwestern Melas basin, Mars: Clues from stratigraphic and morphometric analyses of fans, Icarus, Volume 242, p. 19-37.

J. Williams et al. 2020, Scarp orientation in regions of active aeolian erosion on Mars, Icarus, Volume 335, article id. 113384.

R.D. Wordsworth, The climate of early Mars. Annu. Rev. Earth Planet. Sci. 44, 381–408 (2016)

R. Wordsworth, F. Forget, E. Millour, J.W. Head, J.-B. Madeleine, B. Charnay, Global modelling of the early Martian climate under a denser CO2 atmosphere: water cycle and ice evolution. Icarus 222, 1–19 (2013)

R. Wordsworth, Y. Kalugina, S. Lokshtanov, A. Vigasin, B. Ehlmann, J. Head, C. Sanders, H. Wang, Transient reducing greenhouse warming on early Mars. Geophys. Res. Lett. 44(2), 665–671 (2017)

4. Data Management Plan.

following the NASA Planetary Science Division ROSES Data Management Plan (DMP) Template

1. Overview of the data that will be produced by the proposed project:

We propose to be involved in improving planned data products via generating the following additional science products: Everything in the "Science Products" column of Table 1 in this proposal, specifically Grain-size distributions; River-deposit widths, thicknesses, and radii of curvature (where visible); Bedset-thickness data; Catalog of interbedded craters. Results of analysis of interbedded-crater density; Depth and width of corrugations in the unconformity outcrop; Locally-averaged layer thickness at multiple stratigraphic levels. The chain of reasoning used to generate summary stratigraphic logs (e.g. list of image IDs examined, and specific interpretations made) will also be shared. We will also generate protocols (i.e., detailed self-contained descriptions) for the methods by which the science products of the proposed investigation were obtained from Mars 2020 instrument data products; Source code and instructions for use of all PI-owned/produced software listed in Box 1, plus any additional Jezero-relevant/Mars-2020-relevant code generated by the PI, the Graduate Student Researcher, or the Postdoctoral Researcher that is used in a peer-reviewed scientific publication; and "Figure reproducibility" scripts (a one-click pipeline that output the graphs for published figures in a publication; at least one such script per publication).

2. Data types, volume, formats, and (where relevant) standards:

Data: Comma separated variable (.csv) files (machine-readable format), negligible (i.e., < 0.1 GB) total volume. *Scripts:* Negligible (< 0.01 GB) total volume; in a format readable by a widely used programming language (the PI does not require a specific scientific programming language for people working under his supervision), such as MATLAB, Python, or IDL; plus any plain-text README files needed to understand the relationships between the scripts and any needed input files.

3. **Schedule for data archiving and sharing:**

Simultaneous with publication of results. Intended publication schedule is given in Section 2.5, Work Plan. Publication of results will be at a schedule governed by the Mars 2020 Rules of the Road document which takes precedence over the Work Plan in this proposal. The data behind figures and tables will be available electronically at the time of publication, as supplementary material uploaded with the article.

4. Intended repositories for archived data and mechanisms for public access and distribution:

The Announcement of Opportunity for this call, Appendix C.26 of ROSES, states, "if peer reviewed publications result from these awards, the data behind figures and tables must be available electronically at the time of publication, ideally in supplementary material with the article." The data that will be generated by the proposed investigation is of modest size and of suitable format for release as Supplementary Information in peer-reviewed scientific journals. This plan is specifically endorsed by the Frequently Asked Questions (FAQ) page for ROSES about Data Management Plans (DMPs) as updated for ROSES-2020 (https://science.nasa.gov/researchers/sara/faqs/dmp-faq-roses). Our intent is to publish in AGU

journals (specifically JGR-Planets or GRL). AGU journals do not have a paywall for Supplementary Information.

5. Plan for enabling long-term preservation of the data:
Our plan is to supplementary material in peer-reviewed publications. It is unlikely that a major planetary science journal suitable for publication of Mars 2020 results will become defunct. Nevertheless, as a backup we will also upload the data to the Box repository (https://its.uchicago.edu/uchicago-box/) of the PI's home institution, University of Chicago. The University of Chicago archive complies with NASA's requirement for a "stable and long-term supported data repository." Through membership of the Mars 2020 Team, we will engage in discussion with PDS representatives about possible PDS archiving (likely at the Geoscience Node) as a second backup.

6. Software archiving plan:
The PI-developed source code, specifically ISEE-Mars (Kite et al. 2013b), embedded crater analysis/paleopressure pipeline (Kite et al. 2014/2017), and erosion-rate analysis pipeline (Kite & Mayer 2017), with associated documentation sufficient to enable use of the code, will be made publicly available via NASA GitHub (https://github.com/NASAPlanetary-Science), as encouraged in Section 3.6.1 of Appendix C.1 of the ROSES call. NASA Github is the appropriate repository, following the Section 3.6.1 guidelines, because none of the PI-developed source code is mission-specific. The PI has a copy of the source code of CHIM-XPT (which is used to combine inputs with SOLTHERM), however CHIM-XPT was not generated for a Mars 2020 purpose, nor is the PI free to redistribute the code (which was developed by Professor Mark Reed / University of Oregon), so therefore it is neither practical nor feasible to share the source code. Roughly the same results should be obtained using any commercial or academic reaction transport code (e.g. Toughreact, GWB Pro) given the same thermodynamic database. The SOLTHERM thermodynamic database used for the reaction-transport modeling is already public and widely available.

7. Astromaterials archiving plan:
Not applicable.

8. Roles and responsibilities of team members for data management:
All personnel will carry out data archiving in Years 1-3, primarily via the graduate student and the postdoc working under the PI's direction. The PI will be responsible for archiving his software code. The graduate student and the PI will carry out data archiving in Year 4. If people working under the PI's direction generate software code as part of this investigation (which is not part of the plan, but might reasonably be expected to occur), then they will be responsible for archiving that code via NASA Github under the PI's supervision. There is no charge to the PI for UChicago-specific archiving given the small total volume of the data (<0.1 GB) to be generated as a result of the proposed investigation.

5. Biographical Sketches.

Edwin S. Kite (Principal Investigator).

Appointments:
University of Chicago. Assistant Professor, January 2015 – .
Princeton University. Harry Hess Fellow, 2014.
California Institute of Technology. O.K. Earl Fellow, 2012-2013.

Professional preparation:
Cambridge University (Natural Sciences Tripos – Geological Sciences), B.A. & MSci June 2007
University of California Berkeley (Earth and Planetary Science), Ph.D. December 2011
Advisor: Michael Manga; Thesis topic: "Climate change on ancient Mars."

Awards etc: Greeley Early Career Award in Planetary Science (AGU) 2016.
National Academy of Sciences - Committee on Astrobiology and Planetary Science 2017-
AAAS Newcomb Cleveland Prize 2009 (most outstanding *Science* paper; shared).

Mars papers from the last 3 years (n = 17):
(Mentees working under Kite's supervision underlined)

Heard, A., & **Kite, E.S.**, 2020, "A probabilistic case for a large missing carbon sink on Mars after 3.5 billion years ago," Earth & Planetary Science Letters, 531, 116001.

Holo, S., & **Kite, E.S.**, 2020, "The spatial signature of a changing impactor population for Mars," Icarus, 337, 113447.

Kite, E.S., Mischna, M., Gao, P., Yung, Y., & Turbet, M., 2020, "Methane release on Early Mars by atmospheric collapse and atmospheric reinflation," Planetary & Space Science, 181, 104820.

Warren, A.O., **Kite, E.S.**, Williams, J.-P., & Horgan, B., 2019, "Through the thick and thin: New constraints on Martian paleopressure history 3.8-4 Ga from small exhumed craters," Journal of Geophysical Research – Planets, 121, 2793- 2818.

Stucky de Quay, G., **Kite, E.S.**, & Mayer, D.P., 2019, "Prolonged fluvial activity from channel-fan systems on Mars," Journal of Geophysical Research – Planets, 124, 3119-3139.

Kite, E.S., Mayer, D.P., Wilson, S.A., Davis, J.M., Lucas, A.S., & Stucky de Quay, G., 2019, "Persistence of intense, climate-driven runoff late in Mars history," Science Advances, 5(3).

Kite, E.S., 2019, "Geologic constraints on Early Mars climate," Space Science Reviews, 215: 10.

Kite, E.S., & Melwani Daswani, M., 2019, "Geochemistry constrains global hydrology on Early Mars," Earth & Planetary Science Letters, 524, 115718, 10 pp.

Holo, S.J., **Kite, E.S.**, & Robbins, S.J., 2018, "Mars obliquity history constrained by elliptic crater orientations," Earth & Planetary Science Letters, 496, 206-

Mansfield, M., **Kite, E.S.**, & Mischna, M., 2018, "Effect of Mars atmospheric loss on snow melt potential in a 3.5-Gyr climate evolution model," arXiv:1802.10422, Journal of Geophysical Research – Planets, doi:10.1002/2017JE005422.

Gabasova, L., & **Kite, E.S.**, 2018. "Compaction and sedimentary basin analysis on Mars," Planetary & Space Science, 152, 86-106, doi:10.1016/j.pss.2017.12.021.

Steele, L., **Kite, E.S.**, & Michaels, T.I., 2018. "Crater mound formation by wind erosion on Mars," Journal of Geophysical Research – Planets, 123, 113-130.

Seybold, H.J., **Kite, E.S.**, & Kirchner, J., 2018, "Branching geometry of valley networks on Mars and Earth and its implications for early Martian climate," Science Advances, 4(6), eaar6692.

Kite, E.S., Gao, P., Goldblatt, C., Mischna, M., Mayer, D.P., & Yung, Y., 2017. "Methane bursts as a trigger for intermittent lake-forming climates on post-Noachian Mars," Nature Geoscience, 10, 737-740.

Melwani Daswani, M., & **Kite, E.S**., 2017. "Paleohydrology on Mars constrained by mass balance and minerology of pre-Amazonian sodium chloride lakes: Deep groundwater not required", Journal of Geophysical Research – Planets, 122, 1802-1823,

Kite, E.S., & Mayer, D.P., 2017. "Mars sedimentary rock erosion rates constrained using crater counts, with applications to organic-matter preservation and to the global dust cycle," Icarus, 286, 212-222, doi:10.1016/j.icarus.2016.10.010.

Kite, E.S., Sneed, J., Mayer, D.P., & Wilson, S.A., 2017. "Persistent or repeated surface habitability on Mars," Geophysical Research Letters, 44, 3991-3999.

Selected additional papers on Mars or planetary habitability:

Kite, E.S., Fegley, B., Schaefer, L., & Ford, E.B., 2020, "Atmosphere origins for exoplanet sub-Neptunes," Astrophysical Journal, 891:111 (16pp).

Kite, E.S., Fegley, B., Schaefer, L., & Ford, E.B., 2019, "Superabundance of exoplanet sub-Neptunes" explained by fugacity crisis, Astrophysical Journal Letters, 887:L33.

Kite, E.S., & Ford, E., 2018, "Habitability of exoplanet waterworlds," Astrophysical Journal, 864, 75, 28 pp, doi.org/10.3847/1538-4357/aad6e0.

Kite, E.S., Sneed, J., Mayer, D.P., Lewis, K.W., Michaels, T.I., Hore, A., & Rafkin, S.C.R., 2016. "Evolution of major sedimentary mounds on Mars," JGR – Planets, 121, 2282-2324.

Kite, E.S., Howard, A., Lucas, A., & Lewis, K.W., 2015. "Resolving the era of river-forming climates on Mars using stratigraphic logs of river-deposit dimensions," Earth & Planetary Science Letters, 420, 55-65, doi:10.1016/j.epsl.2015.03.019

Kite, E.S., Howard, A., Lucas, A., Armstrong, J.C., Aharonson, O., & Lamb, M.P., 2015. "Stratigraphy of Aeolis Dorsa, Mars: stratigraphic context of the great river deposits," Icarus, 253, 223-242.

Kite, E.S., Williams, J.-P., Lucas, A., & Aharonson, O., 2014. "Low palaeopressure of the Martian atmosphere estimated from the size distribution of ancient craters," Nature Geoscience, 7, 335-339.

Kite, E.S., Lewis, K.W., Lamb, M.P., Newman, C.E., & Richardson, M.I., 2013. "Growth and form of the mound in Gale Crater, Mars: Slope-wind enhanced erosion and transport," Geology, 41, 543-546

Kite, E.S., Halevy, I., Kahre, M.A., Manga, M., & Wolff, M., 2013a. "Seasonal melting and the formation of sedimentary rocks on Mars," Icarus, 223, 181-210,

Kite, E.S., Lucas, A., & C.I. Fassett, 2013. "Pacing Early Mars river activity," Icarus, 225, 850-855.

Kite, E.S., & R.C.A. Hindmarsh, 2007. "Did ice streams shape the largest channels on Mars?," Geophysical Research Letters, 34, L19202, doi:10.1029/2007GL030530

Field experience: Greece, Spain, England, Scotland, California, Hawaii (volcanism), Pilbara (Archean and Proterozoic environments), Central India (Proterozoic paleobiology), Utah (Mars analogs).